AD-A153 640 ROLLING CONTACT FATIGUE TESTING OF THERMOMECHANICALLY PROCESSED M-50 STEEL(U) NAVAL POSTGRADUATE SCHOOL MONTEREY CA F A BUTTERFIELD DEC 84 1/2

UNCLASSIFIED F/G 20/11 NL

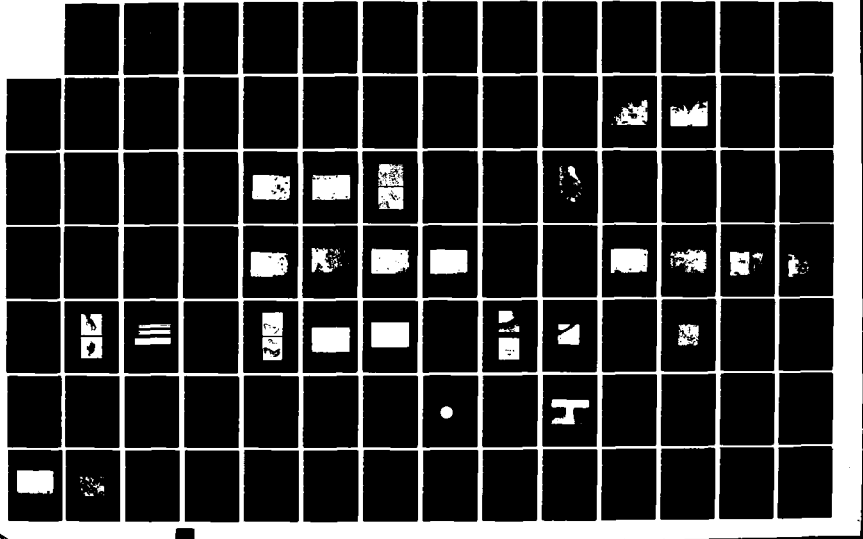

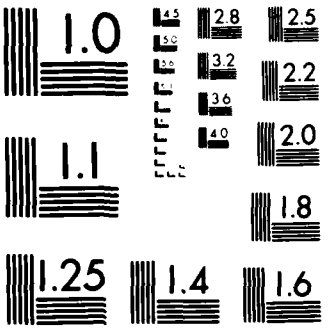

MICROCOPY RESOLUTION TEST CHART
NATIONAL BUREAU OF STANDARDS 1963 A

(2)

AD-A153 640

NAVAL POSTGRADUATE SCHOOL
Monterey, California

DTIC
ELECTE
MAY 1 4 1985
B

THESIS

ROLLING CONTACT FATIGUE TESTING OF THERMOMECHANICALLY PROCESSED M-50 STEEL

by

Fred A. Butterfield, III

December 1984

Thesis Advisor: Terry R. McNelley

Approved for public release; distribution unlimited.

DTIC FILE COPY

85 04 15.032

SECURITY CLASSIFICATION OF THIS PAGE (When Data Entered)

REPORT DOCUMENTATION PAGE	READ INSTRUCTIONS BEFORE COMPLETING FORM
1. REPORT NUMBER	2. GOVT ACCESSION NO. AD-A153640 / 3. RECIPIENT'S CATALOG NUMBER
4. TITLE (and Subtitle) Rolling Contact Fatigue Testing of Thermomechanically Processed M-50 Steel	5. TYPE OF REPORT & PERIOD COVERED Master's Thesis December 1984
	6. PERFORMING ORG. REPORT NUMBER
7. AUTHOR(s) Fred A. Butterfield, III	8. CONTRACT OR GRANT NUMBER(s)
9. PERFORMING ORGANIZATION NAME AND ADDRESS Naval Postgraduate School Monterey, California 93943	10. PROGRAM ELEMENT, PROJECT, TASK AREA & WORK UNIT NUMBERS
11. CONTROLLING OFFICE NAME AND ADDRESS Naval Postgraduate School Monterey, California 93943	12. REPORT DATE December 1984
	13. NUMBER OF PAGES 103
14. MONITORING AGENCY NAME & ADDRESS(if different from Controlling Office)	15. SECURITY CLASS. (of this report) Unclassified
	15a. DECLASSIFICATION/DOWNGRADING SCHEDULE

16. DISTRIBUTION STATEMENT (of this Report)

Approved for public release; distribution unlimited.

17. DISTRIBUTION STATEMENT (of the abstract entered in Block 20, if different from Report)

18. SUPPLEMENTARY NOTES

19. KEY WORDS (Continue on reverse side if necessary and identify by block number)

M-50 steel, rolling contact fatigue, thermomechanical processing, heat treatment, carbides, soluble carbides, insoluble carbides, retained austenite, Weibull distribution, cavitation

20. ABSTRACT (Continue on reverse side if necessary and identify by block number)

The influence on rolling contact fatigue behavior of thermomechanical processing (TMP) to refine grain and soluble carbide size was studied in this work on VIM-VAR M-50 steel. Material was processed (austenitized and warm-rolled) following the procedures developed by Larson, with subsequent austenitization times and temperatures (for final hardening) based on Bres' data. Rolling contact fatigue testing indicates virtual

DD FORM 1 JAN 73 1473 EDITION OF 1 NOV 65 IS OBSOLETE

S/N 0102-LF-014-6601

SECURITY CLASSIFICATION OF THIS PAGE (When Data Entered)

20. ABSTRACT (Continued)

equivalence of the as-received (spheroidize-annealed) and TMP specimens evaluated, with the TMP material clearly no better than the as-received condition in terms of fatigue life. This is believed to be the result of one or both of the following: (a) austenitization (hardening) of TMP material at too long a holding time, with a microstructural equalization occurring between conditions; and (b) voids existing at the ends of insoluble carbides in both as-received and TMP material, which act as possible sites for crack initiation in the matrix.

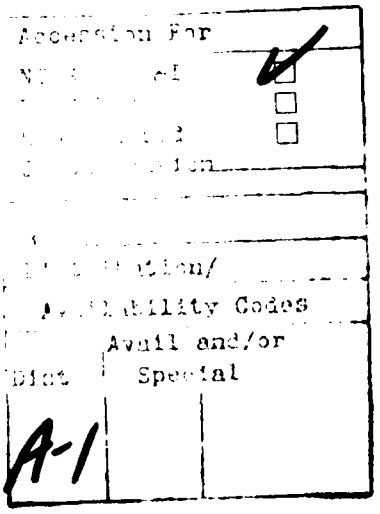

Approved for public release; distribution unlimited.

Rolling Contact Fatigue Testing of Thermomechanically Processed M-50 Steel

by

Fred A. Butterfield, III
Lieutenant, United States Navy
B.S., United States Naval Academy, 1978

Submitted in partial fulfillment of the requirements for the degree of

MASTER OF SCIENCE IN MECHANICAL ENGINEERING

from the

NAVAL POSTGRADUATE SCHOOL
December 1984

Author: Fred A. Butterfield III
Fred A. Butterfield, III

Approved by: T. R. McNelley
Terry R. McNelley, Thesis Advisor

P. J. Marto
Paul J. Marto, Chairman,
Department of Mechanical Engineering

John N. Dyer
John N. Dyer,
Dean of Science and Engineering

ABSTRACT

The influence on rolling contact fatigue behavior of thermomechanical processing (TMP) to refine grain and soluble carbide size was studied in this work on VIM-VAR M-50 steel. Material was processed (austenitized and warm-rolled) following the procedures developed by Larson, with subsequent austenitization times and temperatures (for final hardening) based on Bres' data. Rolling contact fatigue testing indicates virtual equivalence of the as-received (spheroidize-annealed) and TMP specimens evaluated, with the TMP material clearly no better than the as-received condition in terms of fatigue life. This is believed to be the result of one or both of the following: (a) austenitization (hardening) of TMP material at too long a holding time, with a microstructural equalization occurring between conditions; and (b) voids existing at the ends of the insoluble carbides in both as-received and TMP material, which act as possible sites for crack initiation in the matrix.

TABLE OF CONTENTS

I. INTRODUCTION 11

II. EXPERIMENTAL PROCEDURE 16

A. PREPARATION AND INITIAL AUSTENITIZATION . . 16

B. WARM-ROLLING 16

C. PREPARATION FOR ROLLING CONTACT FATIGUE TESTING 17

D. ROLLING CONTACT FATIGUE TESTING 21

E. HARDNESS TESTING 24

F. MICROSCOPY 27

III. RESULTS AND DISCUSSION 29

A. AS-RECEIVED VS. WARM-ROLLED MATERIAL 29

B. HARDENING EFFECT UPON STRUCTURE 36

C. MICROSCOPY OF HARDENED AND TEMPERED SPECIMENS 48

D. ROLLING CONTACT FATIGUE TESTING 54

E. WEIBULL ANALYSIS 64

F. EFFECTS OF RETAINED AUSTENITE 73

IV. COMMENTARY AND CONCLUSIONS 84

V. RECOMMENDATIONS FOR FUTURE WORK 89

APPENDIX A: WEIBULL ANALYSIS DATA 90

LIST OF REFERENCES 99

INITIAL DISTRIBUTION LIST 102

LIST OF TABLES

I. Austenitization Temperatures, by Material Starting Condition 19

II. Hardness of M-50 Steel Specimens After Austenitizing (Before Tempering), Rockwell C . . . 25

III. Hardness of M-50 Steel Specimens, Before Hardening, and After Hardening and Tempering, Rockwell C 26

LIST OF FIGURES

2.1 Rolling Contact Fatigue Test Machine, Naval Air Propulsion Center (NAPC), Trenton, N.J. . . . 22

2.2 Rolling Contact Fatigue Test Machine, Close-Up . 23

3.1 As-Received Material (1270X) 30

3.2 Warm-Rolled (700°C) Material (1270X) 31

3.3 As-Received Material (6000X) 32

3.4 Warm-Rolled (700°C) Material (6000X) 35

3.5 Hardness of Warm-Rolled and As-Received M-50 at Austenitizing Time of Two Minutes, Varying Hardening Temp. (Bres) 38

3.6 Hardness of Warm-Rolled and As-Received M-50 at Austenitizing Temp. 1020°C, Varying Hardening Time (Bres) 40

3.7 Hardness vs. Austenitizing Temperature (Before Tempering) 42

3.8 As-Received, 1006°C (1270X) 44

3.9 As-Received, 1106°C (1270X) 45

3.10 Warm-Rolled (700°C), 1006°C (1270X) 46

3.11 Warm-Rolled (700°C), 1106°C (1270X) 47

3.12 As-Received Material, 1006°C (1270X) 50

3.13 As-Received Material, 1106°C (1270X) 51

3.14 Warm-Rolled (700°C), 1006°C (1270X) 52

3.15 Warm-Rolled (700°C), 1106°C (1270X) 53

3.16 As-Received Material, 1006°C (6000X) 55

3.17 Rolling Contact Test Rods, As-Received: 1106°C (Top), 1006°C (Middle) 56

3.18 "Stereo Pair": As-Received Material, 1006°C (90X) 58

3.19 Sectioned Fatigue Spall: As-Received Material, Austenitized at 1106°C (406X) 59

3.20 Sectioned Fatigue Spall: Warm-Rolled (700°C) Material, Austenitized at 1006°C (406X) 60

3.21 Sectioned Fatigue Spall: As-Received Material, Austenitized at 1006°C (3000X) 62

3.22 Sectioned Fatigue Spall: As-Received Material, Austenitized at 1006°C (6000X) 62

3.23 Sectioned Fatigue Spall: As-Received Material, Austenitized at 1006°C (1500X) 63

3.24 Sectioned Fatigue Spall: As-Received Material, Austenitized at 1106°C (3000X) 65

3.25 Weibull Distribution 66

3.26 Weibull Distribution 67

3.27 Weibull Distribution 68

3.28 Weibull Distribution 69

3.29 Longitudinal Cracking (Cross-Section): Warm-Rolled (750°C) Material, Austenitized at 1066°C . 75

3.30 Warm-Rolled (750°C) Material, Austenitized at 1066°C (1016X) 77

3.31 Intergranular Cracking: Warm-Rolled (700°C) Material, Austenitized at 1106°C (813X) 82

3.32 Fracture Surface of Warm-Rolled (700°C) Material, Austenitized at 1106°C (440X) 83

ACKNOWLEDGMENTS

I wish to express my sincere appreciation to those individuals who have made this research effort possible.

First, I would like to thank my wife Janet and our son, Matthew Jesse, for their love, support, and encouragement, not only during the past nine months of thesis work, but also throughout the entire nine quarters here at the Naval Postgraduate School. I am deeply indebted as well to my thesis advisor and friend, Dr. Terry R. McNelley, for his incalculable guidance and advocacy on my behalf, and for his patience as I floundered through the early stages of this research with question after question. And I would be remiss not to cite Mr. Tom Kellogg, who--as all students of Material Science know--is everybody's right-hand man. Without his valuable technical insight (and insufferable sense of humor), this study would never have gotten off the ground.

I wish to acknowledge Messrs. Dan Popgoshev and Jim O'Donnell of the Naval Air Propulsion Center, Trenton, N.J., through which both financial and physical support for this research were provided. Additionally, Mr. Chris Patton of Hopkins Marine Station, Pacific Grove, California should be commended for his excellent photographic work under the scanning electron microscope. Mr. Erwin V. Zaretsky of NASA's Lewis Research Center, Cleveland, Ohio, was also very

kind to offer his helpful comments and suggestions as I sorted out the results of the microscopy and the Weibull analysis.

Lastly, I thank my God, the Father of my Lord, Jesus Christ. To the extent that I have been able, I have endeavored to honor Him with my thesis work. I am grateful that He alone is the Chief Materials Scientist, the Creator of all life, knowledge, and order; for as the Holy Scriptures so eloquently testify, "He is before all things, and in Him all things hold together" (Colossians 1:17, New International Version).

I. INTRODUCTION

Possible improvements in the capabilities of engine main bearing materials continue to motivate research on steels for application in gas turbines. Engines are now expected to operate in severe environments at higher temperatures and with increased turbine speeds for enhanced performance, as well as with multi-spool configurations for greater efficiency [Ref. 1]. Advances in blading technology include the use of exotic alloying additions and protective oxide coatings, and this aforementioned combination of "hotter, faster, and heavier" places a concomitant burden on bearing metallurgists.

When one speaks of main engine bearing performance, the practical consideration is one of bearing life. This is, for all intents and purposes, the lifespan until failure by fatigue spalling, which is the classical failure mode for rolling-element bearings [Ref. 2]. The foregoing assumes, of course, that the bearing was properly handled, installed, and maintained; that it has been correctly lubricated throughout its lifetime; and that it was not subjected to abuse by either the elements or unqualified operators [Ref. 3]. Thus, the primary objective is to increase the fatigue life of the bearing material, and specifically its life in terms of rolling contact fatigue.

One approach, developed by Larson [Ref. 4] for M-50 steel, is thermomechanical processing (TMP), a two-step technique aimed at producing a microstructural enhancement which may lead to an increase in rolling-element life. Briefly, the TMP consists of a high-temperature austenitization to dissolve soluble carbides, followed by air-cooling, which results in a fine, supersaturated martensitic matrix with newly-precipitated (and refined) soluble carbides. Secondly, the material is reheated and warm-rolled at 0.5 to 0.65 of its absolute melting temperature to induce recrystallization without allowing for excessive grain growth, thereby yielding a refined ferrite grain size.

According to fracture mechanics theory, this will give the material improved fracture toughness. The refinement of the ferrite grains enhances fracture resistance by two means: (a) pre-existing cracks in the matrix will be smaller (due to the smaller grain size), and will require a higher external stress for propagation to occur; and (b) there will be increased grain boundary area in the refined structure, meaning more obstacles in the path of a propagating crack [Ref. 1]. Carbide refinement provides two beneficial effects as well: (a) smaller carbides are not as effective as stress raisers in the matrix as are massive carbides, and are less likely to become sites for crack initiation; and (b) a fine dispersion of carbides as a classical strengthening mechanism. These homogeneously-distributed carbides "pin"

grain boundaries, thus inhibiting grain growth, and also result in secondary hardness via precipitation-hardening during tempering following the final heat treatment.

It must be noted, however, that although the microstructural refinement should result in an improvement of fracture toughness, this is not necessarily synonymous with an enhancement of rolling contact fatigue resistance. This caveat is particularly germane when the associated failure mechanism (e.g., fatigue spalling) is not as well understood, which is the case here. Hence, the need exists to validate our assumptions with this type of mechanical testing.

The material used in this research, AISI M-50 steel, is the aircraft industry's alloy of choice. It is presently specified by virtually all major U.S. gas turbine engine manufacturers for use as their main shaft bearings material [Ref. 3]. Although tool steels account for less than two tenths of one percent of total steel tonnage produced per annum in the United States, their value per pound is about fifty times that of the high-tonnage steels [Ref. 5]. The explanation for this is found in both their heavy degree of alloying, and their specialty applications. Tool steels such as M-50 are especially appropriate for gas turbine bearing usage due to their excellent resistance, not only to wear (for economical life) and to deformation or breaking under

high loading conditions, but also to softening at elevated temperatures.

This latter feature, incidently, is the reason why AISI 52100 steel, long a bearing industry standard material, cannot be used in a gas turbine engine; it will soften in situ at the normal operating temperatures of the engine, threatening a premature failure of the load-bearing component.

The nominal composition (in weight percent) of M-50 steel is given as follows:

C	Mn	Si	Cr	Mo	V
0.80	0.30	0.25	4.10	4.25	1.10

An extensive discussion is devoted to the carbides present in M-50 by Bridge, et al. [Ref. 6]. A brief summary of their relevant findings is reported below under the Results and Discussion chapter. The principal alloying elements in M-50 are chromium, molybdenum, and vanadium. Chromium is a relatively low-cost addition which increases the hardenability of the alloy, and also results in the formation of the soluble carbide $Cr_{23}C_6$, which provides good wear resistance. "M" type (high speed) tool steels are so designated because of their high molybdenum content; a hard carbide, Mo_6C, is produced which, upon tempering, precipitates as fine particles in the martensite and forms the basis for secondary hardening. Vanadium is an expensive element which forms the hard, insoluble carbide VC, an extremely tenacious particle

which also contributes to the excellent wear resistance of the alloy [Refs. 5 and 7].

The material is subjected to VIM-VAR processing. That is, it is vacuum induction melted (VIM) in an induction furnace in which the crucible, heating coil, and ingot mold are enclosed in a vacuum chamber. The steel is then vacuum arc remelted (VAR) in a consumable electrode furnace under a vacuum or an inert gas. This steelmaking process ensures a high-quality product containing only minimal amounts of gas porosity and nonmetallic inclusions [Ref. 8].

II. EXPERIMENTAL PROCEDURE

A. PREPARATION AND INITIAL AUSTENITIZATION

Two approximately six-inch lengths of steel were cut from the 1.75 inch (4.5 cm) diameter M-50 round stock. This "as-received" material was left in a spheroidize-annealed condition by the manufacturer. To commence thermomechanical processing and back the material out of its as-received condition, initial austenitization was accomplished in a high-temperature electrical box furnace (silicon carbide heating elements) following the procedures developed by Larson [Ref. 4]. The steel was pre-heated at 850°C (1562°F) for two hours, and then austenitized at 1150°C (2102°F), also for two hours. This was followed by a stabilizing quench in a furnace at 620°C (1148°F) for two to three minutes, until the glow had disappeared. Then, the specimens were allowed to air-cool to ambient temperature [Ref. 9]. Throughout the austenitization, each length was individually wrapped in nickel foil to prevent decarburization, with titanium sponge added as a deoxidant.

B. WARM-ROLLING

The lengths of austenitized M-50 steel were taken to the Lawrence Berkeley Laboratories, Berkeley, California, for warm-rolling. After heating to 700°C (1292°F) in an

electrically-fired box furnace, the specimens were rolled in a two-high flat mill, with intermediate reheating to 700°C between each pass, to a rough shape about one inch (2.5 cm) square. Then, the lengths of M-50 were rolled in a two-high bar mill, again with reheating between passes, to a rounded-corner square shape of 0.625 inch (1.6 cm) per side.

This same procedure was followed for two additional lengths of spheroidize-annealed M-50 steel, with the exception that warm-rolling was accomplished at a temperature of 750°C (1382°F).

C. PREPARATION FOR ROLLING CONTACT FATIGUE TESTING

Rolling contact fatigue rods were machined from the two warm-rolled conditions (700 and 750°C) and the as-received stock. Each rod was cylindrical in shape, 0.375 inch (9.5 mm) in diameter and about four inches long. It is noted that the warm-rolled material was slightly easier to machine, in that it offered less resistance to the lathe operator and produced a smoother surface.

The preferred method for austenitization of steels is to heat treat in molten salt baths, as this results in rapid, uniform heating and minimizes undesirable decarburization. Since the Naval Postgraduate School currently lacks the facilities to conduct salt bath heat treatment, however, this process was done by a private metals heat treating contractor in the south San Francisco Bay area.

The rods were austenitized (hardened) in salt baths according to the following heat treatment scheme [Ref. 9]: specimens were pre-heated in molten salt at 845°C (1553°F), followed by austenitization in salt at a temperature between 1006°C (1843°F) and 1106°C (2023°F), using a standard hardening holding time of five minutes. The samples were then quickly transferred to a quench salt bath and held there only long enough to attain bath temperature (stabilize), but no more than two to three minutes, especially when the salt bath was agitated. The test rods were then cooled in air to room temperature.

Austenitization temperatures chosen, by material starting condition, are shown in Table I. The hardening temperatures were chosen according to data generated by Bres [Ref. 1]. The highest austenitizing temperature, 1106°C, is the industry's standard, since it allows for complete solutioning of all soluble carbides. By contrast, the lowest temperature, 1006°C, was selected--albeit arbitrarily--so that the effects of undissolved soluble-type carbides could be observed in rolling-element fatigue. This latter austenitizing temperature, however, is still high enough to give the material sufficient hardness so as to perform adequately in a rolling contact test. The intermediate temperatures, 1036 and 1066°C, were employed at a later point in the research to investigate the presence of retained austenite in the as-quenched

Table I

Austenitization Temperatures, by Material Starting Condition

Condition (Rolling Temperature)	Austenitizing Temperature
As-received	1006°C
As-received	1106°C
Warm-rolled (700°C)	1006°C
Warm-rolled (700°C)	1106°C
Warm-rolled (750°C)	1106°C
Warm-rolled (700°C)	1036°C
Warm-rolled (750°C)	1036°C
Warm-rolled (700°C)	1066°C
Warm-rolled (750°C)	1066°C

specimens, evidenced by longitudinal cracking which occurred upon tempering the warm-rolled rods austenitized at 1106°C.

The hardened rods were then subjected to a five-step tempering cycle [Ref. 9], with each phase being two hours long: freezing at -120°F (-84°C), tempering to 1000°F (538°C), freezing, tempering, and tempering again. The specimens were permitted to return to room temperature between phase of the tempering cycle. Freezing was conducted to promote the transformation of retained austenite to untempered martensite by pushing the material below its martensite finish temperature. The actual temperature was somewhat lower than prescribed: -146°F (-99°C). This was a result of the medium chosen in which to freeze the specimens (acetone in liquid nitrogen), although the lower temperatures had neither a beneficial nor a detrimental effect. Acetone freezes at -140°F (-95°C), while the temperature of liquid nitrogen is -320°F (-196°C). Tempering itself was conducted in an electric box furnace with automatic temperature control.

The rolling contact fatigue test rods were sent to the Naval Air Propulsion Center (NAPC), Trenton, N.J., for finish grinding. This removes the thin, decarburized surface layer which inevitably results from an austenitizing heat treatment (even in molten salt). The test rods were given a surface finish of four to eight microinches RMS.

D. ROLLING CONTACT FATIGUE TESTING

NAPC conducted rolling contact fatigue evaluation on site. The rolling contact fatigue tester which was used (Figure 2.1) is a simple device which generates fatigue spalls that are similar to those occuring in actual rolling-element bearings. Figure 2.2 shows a close-up of a test rod mounted in a precision collet (similar to the chuck on a lathe). The test rod is rotated by a small electric motor; the rod in turn drives two hemispherically ground disks which are rimmed with hardened M-50 steel. The hardness of the roller material is comparable to that of the test rod, and is surface finished to between eight and twelve microinches RMS. These disks load against the test rod and provide resistance (in the form of friction) to its rotation. A drip feed system provides lubrication, which is maintained at a constant rate of flow by a needle valve assembly. The lubricant used in the test was MIL-L-23699, a synthetic base-stock ester fluid which is the U.S. Navy's standard lubricating oil for gas turbine engines. An accelerometer is mounted on the load wheel yokes, acting as a vibration pick-up which senses a test rod failure (i.e., a fatigue spall) and subsequently stops the drive system. A technician then records the number of stress cycles until failure occurred and resets the rod on a different track, ensuring a track separation of about

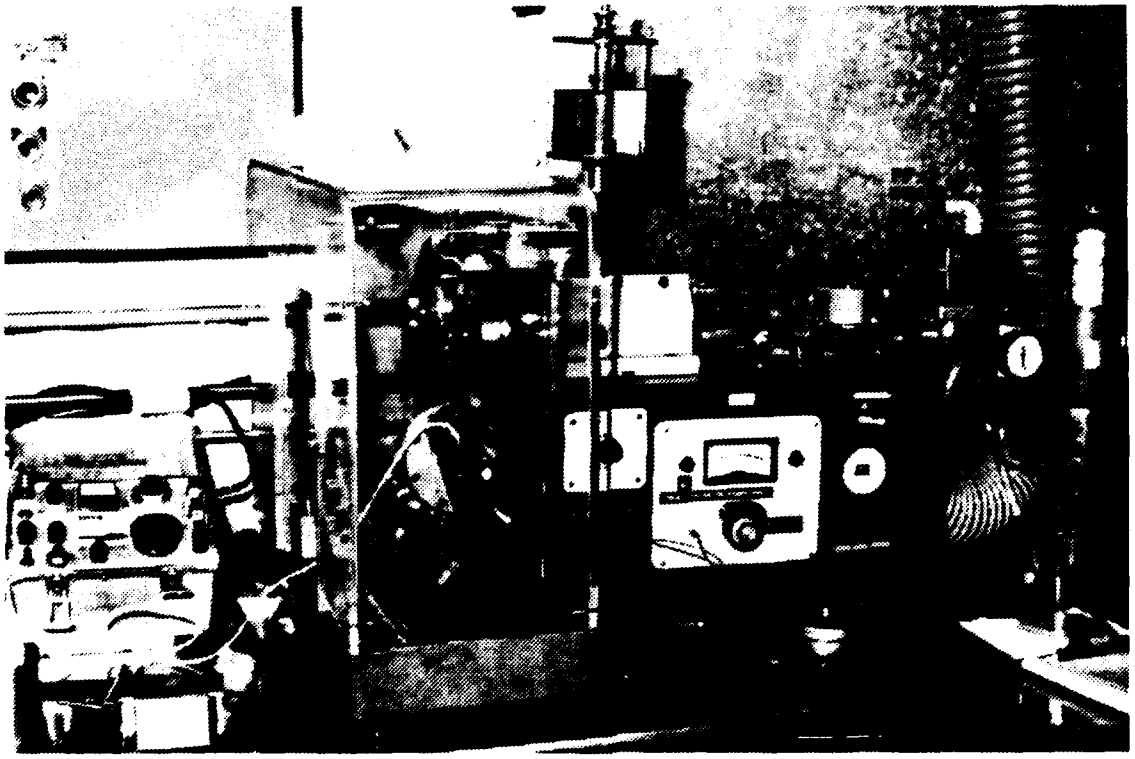

Figure 2.1 Rolling Contact Fatigue Test Machine, Naval Air Propulsion Center (NAPC), Trenton, N.J.

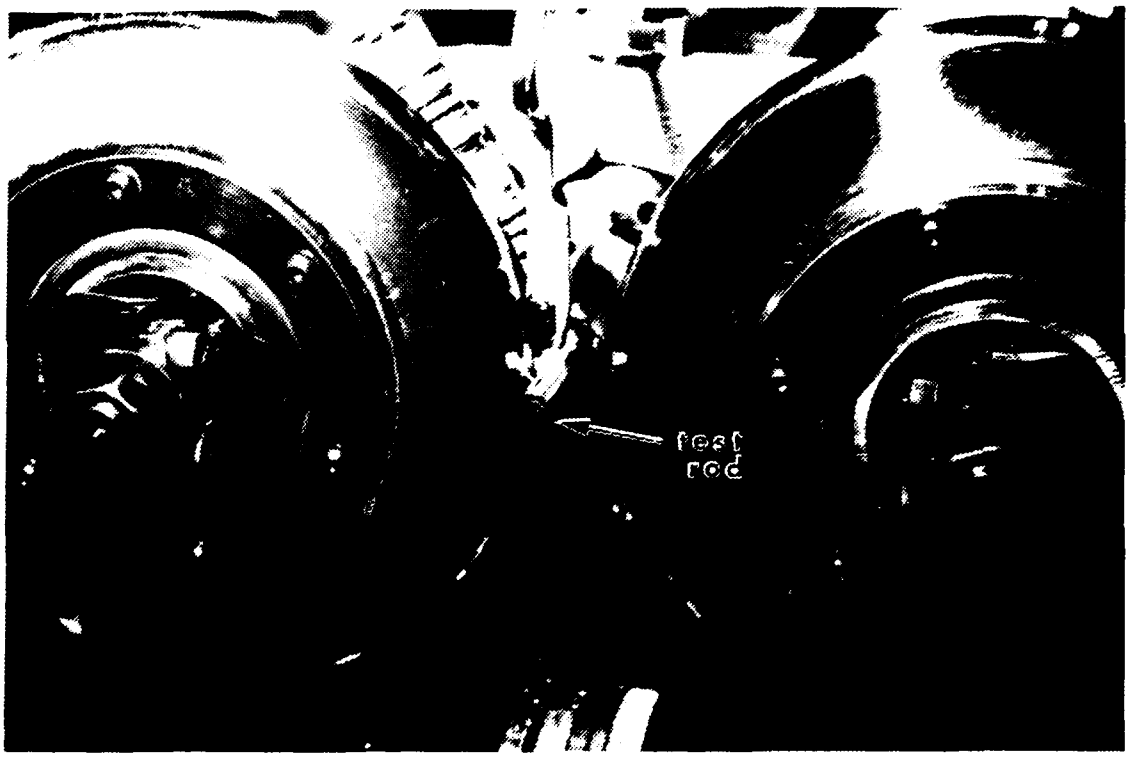

Figure 2.2 Rolling Contact Fatigue Test Machine, Close-Up

0.125 inch (3.2 mm) in order to preclude interactions between tracks [Ref. 10].

The following standard test conditions were observed throughout the research:

(a) oil temperature--ambient;

(b) test rod temperature--ambient;

(c) test rod rotating speed--35,000 to 36,000 rpm (583 to 600 rps);

(d) applied load--1467.84 N (300 lbf);

(e) maximum hertz stress--4.826 GPa (700 ksi); and

(f) lubricant flow rate--20 drops/min.

Testing on a track continued until failure by fatigue spalling occurred, either on the test rod or the load disk [Ref. 10]. In one case, however, the test was discontinued due to an excessive number of stress cycles.

E. HARDNESS TESTING

Hardness data was taken on a Wilson Model 1-JR Rockwell hardness tester. Samples were hardness-tested in the as-received and warm-rolled conditions at three points in the heat treatment process (a) before hardening, (b) after austenitizing but before tempering, and (c) after tempering. The results of test (b) above are given in Table II, while test data for (a) and (c) are reflected in Table III. The Rockwell C scale and a diamond-cone Brale indenter were used in the testing. Six readings were taken per sample, and an arithmetic mean and standard deviation for the data were

Table II

Hardness of M-50 Steel Specimens After Austenitizing (Before Tempering), Rockwell C

Condition (Rolling) Temperature	Austenitizing Temperature	Average Hardness	Standard Deviation
As-received	1006°C	65.1	0.82
As-received	1036°C	64.9	0.31
As-received	1066°C	64.4	0.80
As-received	1106°C	64.8	0.23
Warm-rolled (700°C)	1006°C	65.0	0.70
Warm-rolled (700°C)	1036°C	64.9	0.65
Warm-rolled (700°C)	1066°C	65.1	0.32
Warm-rolled (700°C)	1106°C	63.4	0.88
Warm-rolled (750°C)	1006°C	65.8	0.48
Warm-rolled (750°C)	1036°C	64.5	0.31
Warm-rolled (750°C)	1066°C	65.9	0.86
Warm-rolled (750°C)	1106°C	63.0	0.20

Table III

Hardness of M-50 Steel Specimens, Before Hardening, and After Hardening and Tempering, Rockwell C

Condition (Rolling) Temperature	Austenitizing Temperature	Average Hardness	Standard Deviation
As-received	--	10.3	0.92
Warm-rolled (700°C)	--	34.9	1.53
Warm-rolled (750°C)	--	30.3	1.25
As-received	1006°C	59.7	0.42
As-received	1106°C	58.4	0.91
Warm-rolled (700°C)	1006°C	58.9	0.63
Warm rolled (700°C)	1106°C	62.3	0.25
Warm-rolled (750°C)	1106°C	62.5	0.41
Warm-rolled (700°C)	1036°C	58.8	0.29
Warm-rolled (750°C)	1036°C	58.0	0.67
Warm-rolled (700°C)	1066°C	57.3	0.45
Warm-rolled (750°C)	1066°C	55.8	1.25

then calculated. Since the shape of the rolling contact test rod is that of a cylinder, it was necessary to apply a correction value for the workpiece; these corrections were added to the Rockwell dial-gage readings, as hardness was measured on the outer (convex) surface [Ref. 11].

F. MICROSCOPY

Specimens were cut from the test rods, mounted in phenolic compound, and polished. Vilella's reagent (5 ml HCl, 1 g picric acid, and 100 ml 95% ethanol) was chosen as the etchant because of its qualities for contrast etching in untempered and tempered martensite [Ref. 12]. Initially, the reagent was diluted with an equal quantity of 95% ethanol in order to give more control during etching (i.e., to slow down the reaction); etching times of twenty and thirty seconds were used. Eventually, however, when greater familiarity was gained with the etchant, undiluted Vilella's reagent was utilized, with etching times from twelve to fifteen seconds.

Optical microscopy was conducted under a Zeiss Universal Photomicroscope using Kodak Panatomic-X 35 mm film (FX135-36), ISO 32. Scanning electron microscopy was done on two machines; a Hitachi S-450 SEM at the Hopkins Marine Station, Pacific Grove, California; and, briefly, the Naval Postgraduate School's Cambridge S4-10 Steroscan SEM.

Polaroid Type 52 Polapan 4X5 land film, 400 ASA, was used for all scanning electron photomicrography.

III. RESULTS AND DISCUSSION

A. AS-RECEIVED VS. WARM-ROLLED MATERIAL

Before hardening, the microstructures of both the as-received and warm-rolled products were examined using both optical and scanning electron microscopy. Under the optical microscope at 1270X, the as-received material (Figure 3.1) shows well-defined grains and large, irregularly-shaped insoluble (MC and M_2C) carbides. These larger residual carbides cannot be dissolved without melting of the alloy. Soluble, or temper, carbides cannot be resolved at this magnification. The dramatic effect on grain size resulting from warm-rolling is seen in Figure 3.2: the individual grain boundaries are no longer visible, though the insoluble carbides retain their large, irregular morphology. From this micrograph, it cannot be determined whether any insoluble carbide refinement has been accomplished, although the rolling has caused these carbides to appear as elongated "bands" within the matrix, parallel to the rolling direction of the material. As with the as-received material, temper carbides cannot be seen.

Under the scanning electron microscope at a magnification of 6000X (Figure 3.3), the as-received material exhibits the large, insoluble carbides and also the smaller temper carbides. These latter, soluble carbides are

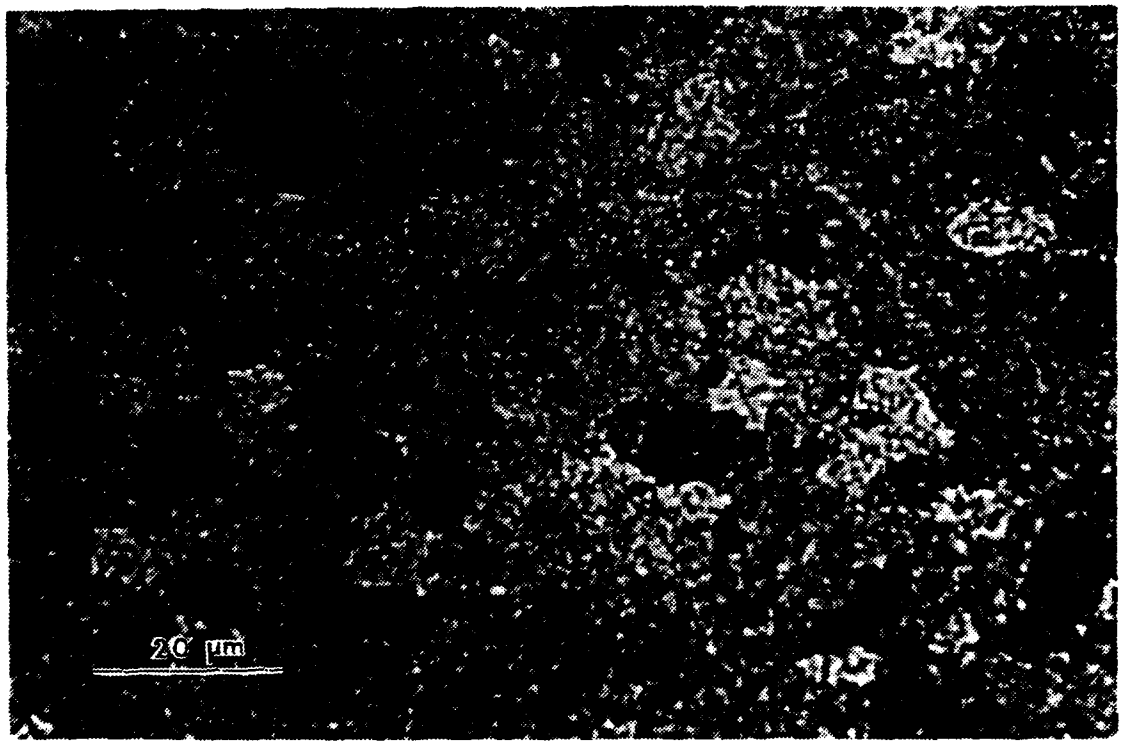

Figure 3.1 As-Received Material (1270X)

Figure 3.2 Warm-Rolled (700°C) Material (1270X)

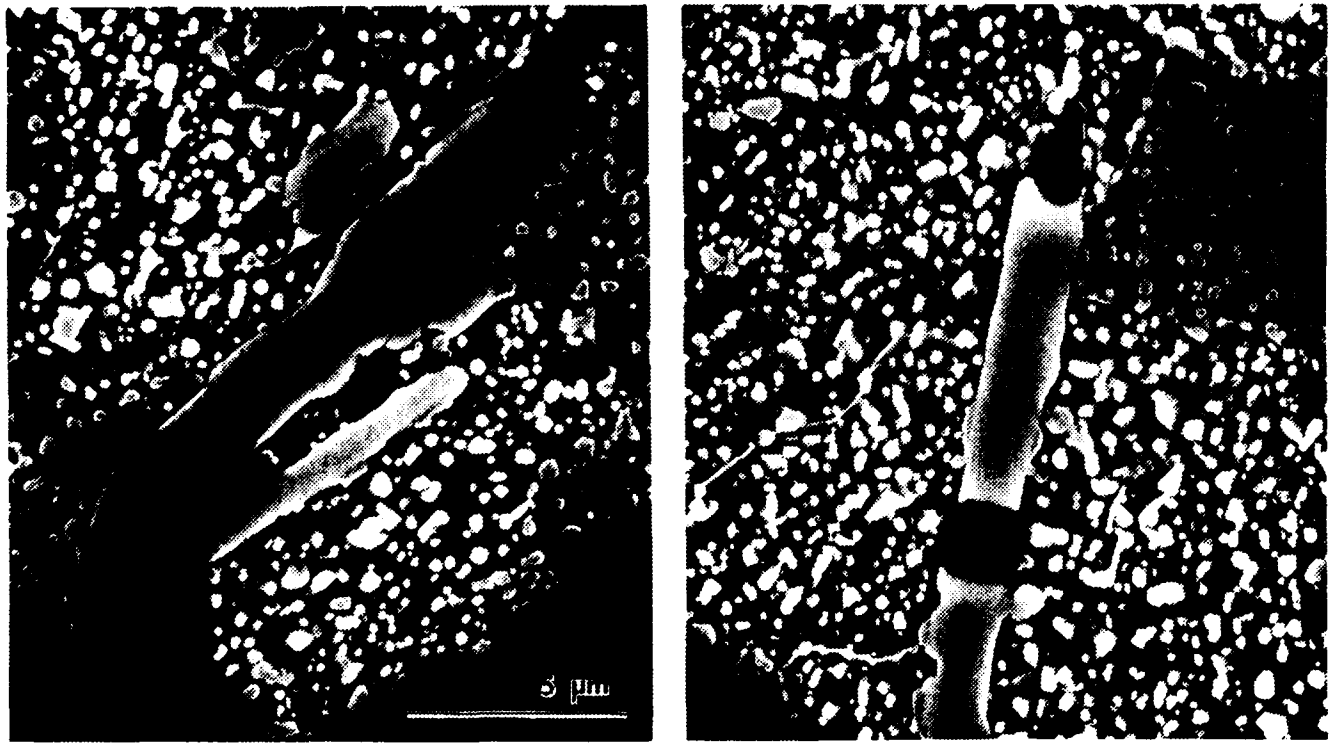

Figure 3.3 As-Received Material (6000X)

spheroidized and homogeneously dispersed in the matrix. The grain boundaries of the material are also observed as contrasting light and dark areas within the matrix. Neither the soluble nor the insoluble carbides "respect" the grain boundaries of the material, as carbide nucleation appears to favor no particular location.

Observe as well the small holes, or voids, at the ends of the insoluble carbides. This is cavitation which is presumably caused by the hot rolling of the steel into bar stock when manufactured. This phenomenon was observed (under the scanning electron microscope only) in virtually every sample of this material, both before and after thermo-mechanical processing, and regardless of the heat treatment scheme followed. Since the voids exist "in the shadow" of the insoluble carbides, their presence using optical microscopy was, understandably, not visible. It is thought that, during the rolling, the insoluble carbides behave as hard, undeformable particles in a relatively soft matrix. Thus, cavitation occurs at the ends of these residual carbides, analogous to the manner in which a high and low pressure zone exists at the upstream and downstream ends, respectively, of an obstruction in a flow stream. This is a significant finding which may have important ramifications with regard to the performance of M-50 steel in rolling-element applications, a point emphasized below in the discussion of the Weibull analysis.

Figure 3.4 shows the warm-rolled material at the same magnification (6000X), and there it is observed that the soluble carbides clearly have been refined in size, although there is no discernable effect upon the insoluble carbides. The temper carbides again show a fine dispersion in the matrix, with neither soluble nor insoluble carbides demonstrating a proclivity to segregate. Areas of sharp grain boundary definition are visible to a lesser extent due to the obvious refinement of the grain size. These are represented by smaller areas of varying contrast in the structure. Cavitation is again observed, although it is less pronounced than in the previous (as-received) specimens.

The results of the microscopy performed on the prehardened material confirms the work done by Larson with regard to thermomechanical processing of M-50 steel [Ref. 4] with only one exception: the large residual carbides are reduced in size only by a small amount, if at all. In both the as-received and warm-rolled material, large insoluble carbides could be found which were representative of the carbide size throughout the structure. This, qualitatively, makes the task of assessing their degree of refinement difficult if not impossible. Also, it stands in sharp contrast to the order-of-magnitude refinement produced on the temper carbides in the warm-rolled matrix. Larson concluded that this refinement was brought about by at least two factors. First, the dissolved carbides are precipitated

Figure 3.4 Warm-Rolled (700°C) Material (6000X)

as a fine temper carbide dispersion from a supersaturated martensite. Secondly, recrystallization during the warm-rolling provides nucleation sites for the enhancement of precipitation. Also, deformation acts to shear larger precipitates, reducing them in size to finer particles. The efficacy of the warm-rolling in breaking up the hard, insoluble carbides, in light of the results of current optical and scanning electron microscopy, is doubtful.

In addition, these results on M-50 regarding the refinement of soluble carbides by thermomechanical processing also supports the work by McNelley et al. [Ref. 13] on AISI 52100 steel. There, too, the starting structure (coarse spheroidal carbides of the as-received condition) was refined during the thermomechanical process. In 52100 steel, however, all of the carbides could be driven into solution. The combination of heat treatment and warm working produced an ultrafine ferrite grain size with a homogeneous dispersion of spheroidal (temper) carbides, and matches the results obtained with M-50 except for the presence of the insoluble (and apparently unrefineable) residual carbides in the latter.

B. HARDENING EFFECT UPON STRUCTURE

The hardening response of M-50 steel upon thermomechanical processing was thoroughly documented by Bres [Ref. 1]. This work, in part, showed that, up to a temperature of approximately 1100°C (2012°F), the warm-rolled samples

demonstrated higher hardness (Rockwell C) than did the conventional, spheroidize-annealed (as-received) condition. Beyond 1100°C, the two structures came together in terms of hardness until they both experienced a slight softening starting at about 1125°C (2057°F) (Figure 3.5).

The increase in hardness as a function of austenitizing temperature is simply a reflection of the increasing quantity of free carbon in the matrix as the carbides undergo dissolution. The carbides in annealed M-50 have been found to be $M_{23}C_6$, M_6C, M_2C, and MC [Ref. 6]. The first two, $M_{23}C_6$ and M_6C, are soluble carbides whose solvus temperatures are 993°C (1820°F) and 1088°C (1990°F), respectively. The remaining carbides, M_2C and MC, are residual and cannot be dissolved without causing liquation of the steel. It can easily be seen that--up to the higher solvus temperature (1100°C)--the soluble carbides are not yet completely dissolved, and therefore hardness differences exist. Upon attainment of this temperature, however, no more carbon is being taken into solution, and the two curves coincide. The subsequent softening of both materials can be explained both as a manifestation of increasing grain size with temperature and the higher content of retained austenite in the specimens [Ref. 14].

Additionally, Bres showed that, by holding austenitizing temperature at a constant value (in this case, 1020°C (1868°F)) and varying the heat treatment time from two to

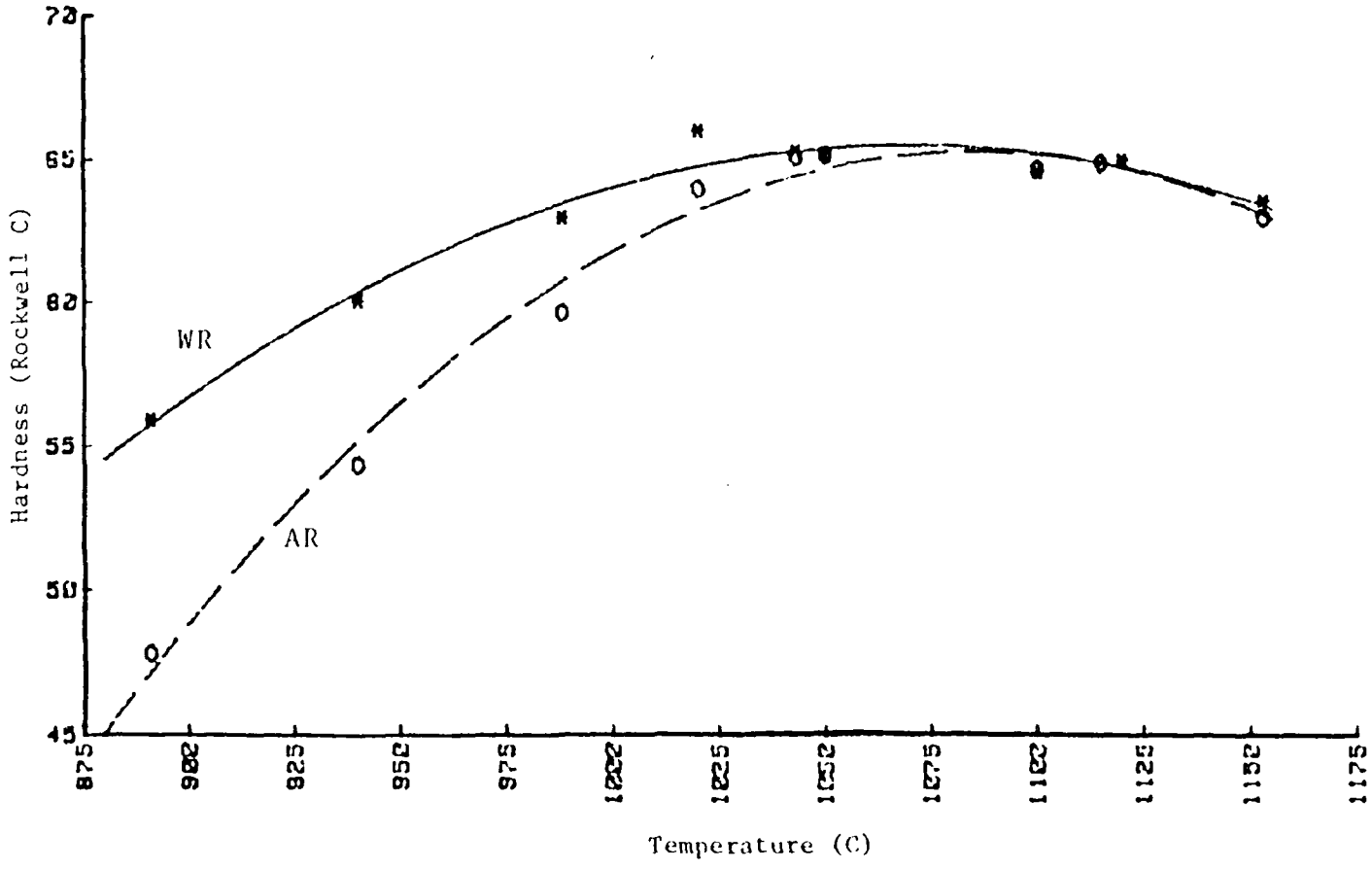

Figure 3.5 Hardness of Warm-Rolled and As-Received M-50 at Austenitizing Time of Two Minutes, Varying Hardening Temp. (Bres)

twenty minutes, the warm-rolled M-50 had a notably higher hardness than the spheroidize-annealed sample for austenitizing times up to five minutes. For the longer austenitizing times (five minutes or greater), the two conditions roughly equalized in hardness (Figure 3.6). The fact that these two curves converge at the longer hardening times is indicative of the speed at which the soluble carbides are completely taken into solution when held at a relatively high austenitizing temperature [Ref. 1].

Alternately stated, heat treatment (i.e., thermomechanical processing) of the warm-rolled M-50 always yielded a product that is at least as hard as the as-received material. And, at either shorter austenitizing times or lower austenitizing temperatures, the warm-rolled material is significantly harder than the as-received steel given an identical heat treatment.

Bres used test coupons of as-received and warm-rolled M-50 steel which were, in both cases, about 2.5 mm (0.1 inch) thick; a standard austenitizing time of two minutes was chosen. In the current work, the rolling contact test rods were machined to a diameter of 0.375 inch (9.5 mm). Since this was--at a maximum--approximately 3.8 times the thickness of the coupon used in the previous study, a standard austenitizing time of five minutes was arbitrarily chosen, with the expectation that this holding time would allow for complete through-hardening of the material upon

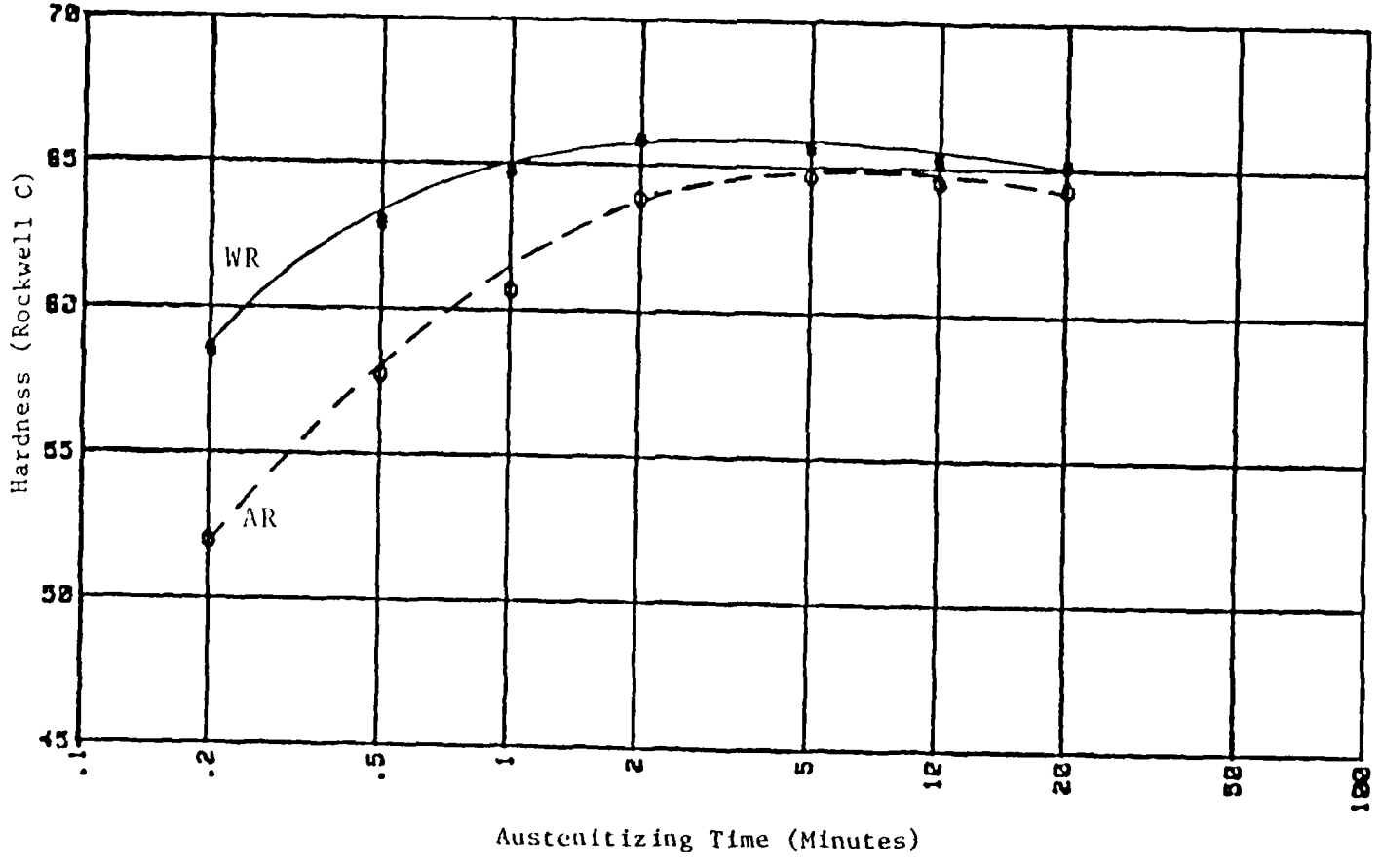

Figure 3.6 Hardness of Warm-Rolled and As-Received M-50 at Austenitizing Temp. 1020°C, Varying Hardening Time (Bres)

austenitization. The hardness results for the as-received and two warm-rolled conditions, heat treated at four different temperatures, are given in Table II. These hardness readings, taken on the Rockwell C scale, were obtained before the material had been tempered. Hardness measurements taken on samples of this material both before austenitizing and also after hardening and tempering appear in Table III.

The remarkable similarity in the hardness data, especially between the lowest and highest austenitizing temperatures, was not anticipated. Note that the minimum and maximum hardness readings--63.0 and 65.9, respectively--differ by less than three Rockwell C numbers. The relatively high degree of statistical uncertainty evidenced by the (large) computed values of the standard deviation leads one to conclude that the hardness for all specimens is essentially uniform, with only a slight softening observed at the highest austenitizing temperature for each condition, most likely a function of the increase in grain size and greater amount of retained austenite. These data are also represented graphically in Figure 3.7, where the essentially constant hardness--even with increased austenitizing temperature--is clearly seen. This is particularly true in the as-received and warm-rolled (700°C) conditions, which show little scatter at the three lower temperatures.

Optical microscopy was consistent with the results of the hardness testing above. Turning to the micrographs

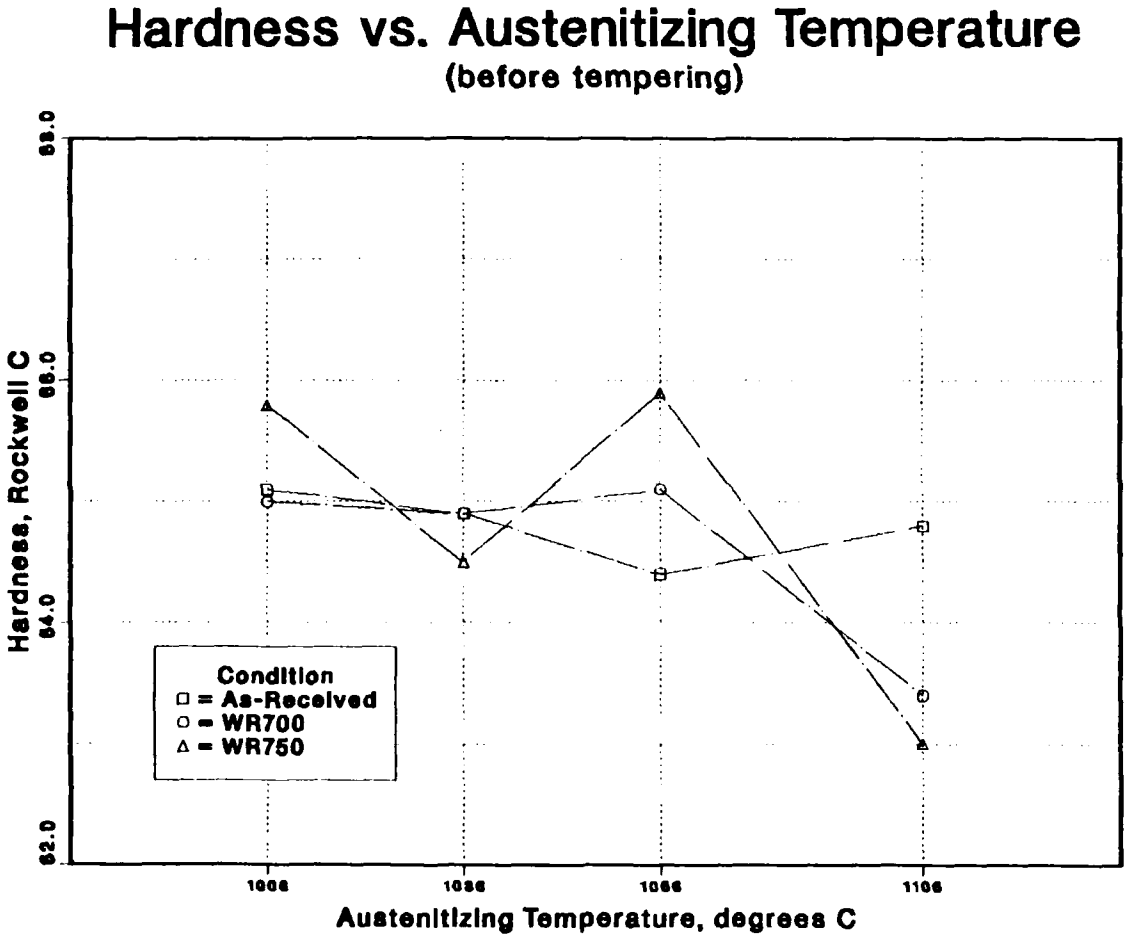

Figure 3.7 Hardness vs. Austenitizing Temperature (Before Tempering)

(1270X) of these material (Figure 3.8 through 3.11), one is struck by the similarities of the microstructures rather than by the differences. Figures 3.8 and 3.10 represent the as-received and the warm-rolled (700°C) material, respectively, at 1006°C. The two micrographs are nearly identical, with no apparent distinction in grain size, amount of retained austenite, or residual carbide size and dispersion. Figures 3.9 and 3.11, depicting the same material conditions at the highest austenitizing temperature employed (1106°C), show the same characteristics. Though the increase in grain size, particularly in the warm-rolled material (Figure 3.11) is clear, as are the indications of a higher degree of retained austenite (relative to Figures 3.8 and 3.10), the similarity of features is still the dominant characteristic. Note also that in all four micrographs there is no clear refinement of the insoluble carbides. With such similarities between the microstructures, it is not difficult to see why the hardness readings are nearly identical as well.

A conclusion is unmistakable: five minutes at the austenitizing temperature is simply too long a time, and has resulted in coarsening of the rolled structure to the point that it is little different from the as-received condition. This nullifies the refinement resulting from the thermo-mechanical processing, bringing both the microstructures and the hardnesses (which, of course, simply reflect the

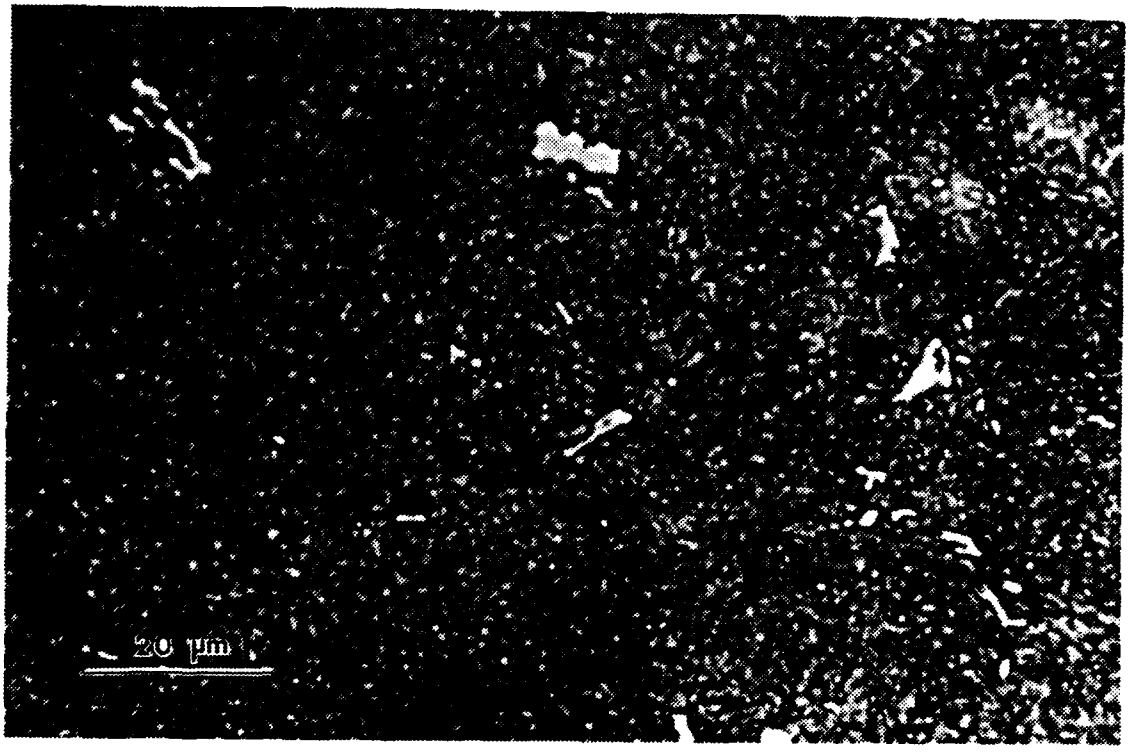

Figure 3.8 As-Received, 1006°C (1270X)

Figure 3.9 As-Received, 1106°C (1270X)

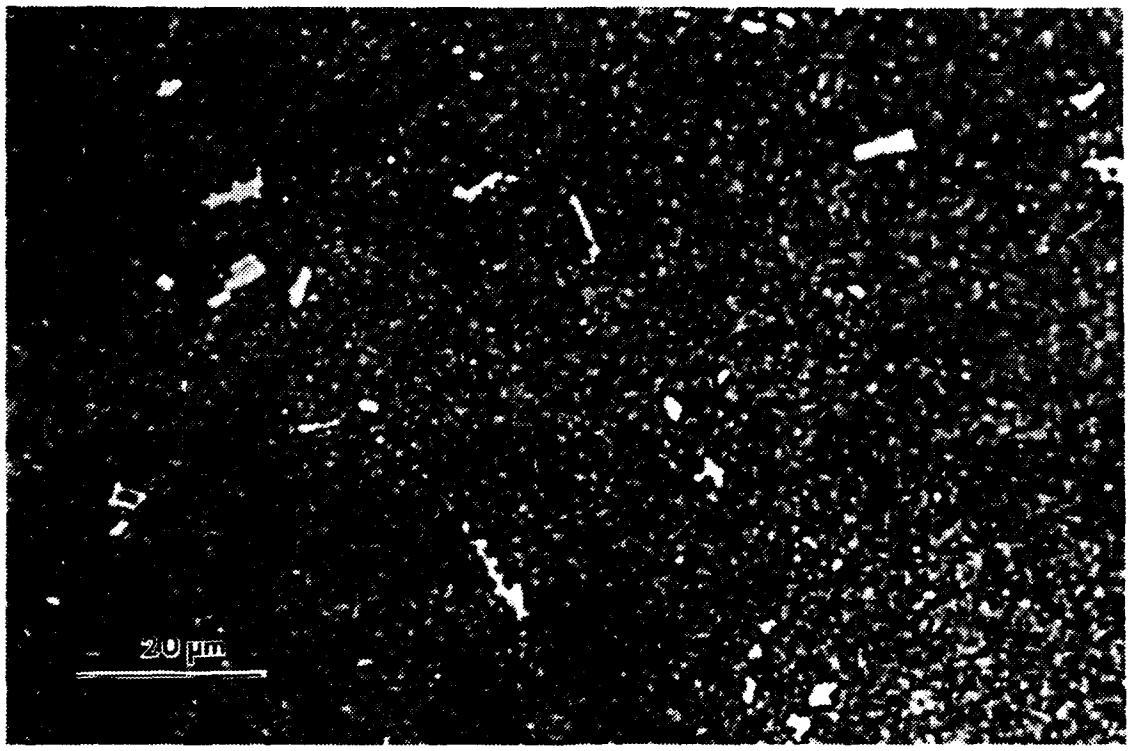

Figure 3.10 Warm-Rolled (700°C), 1006°C (1270X)

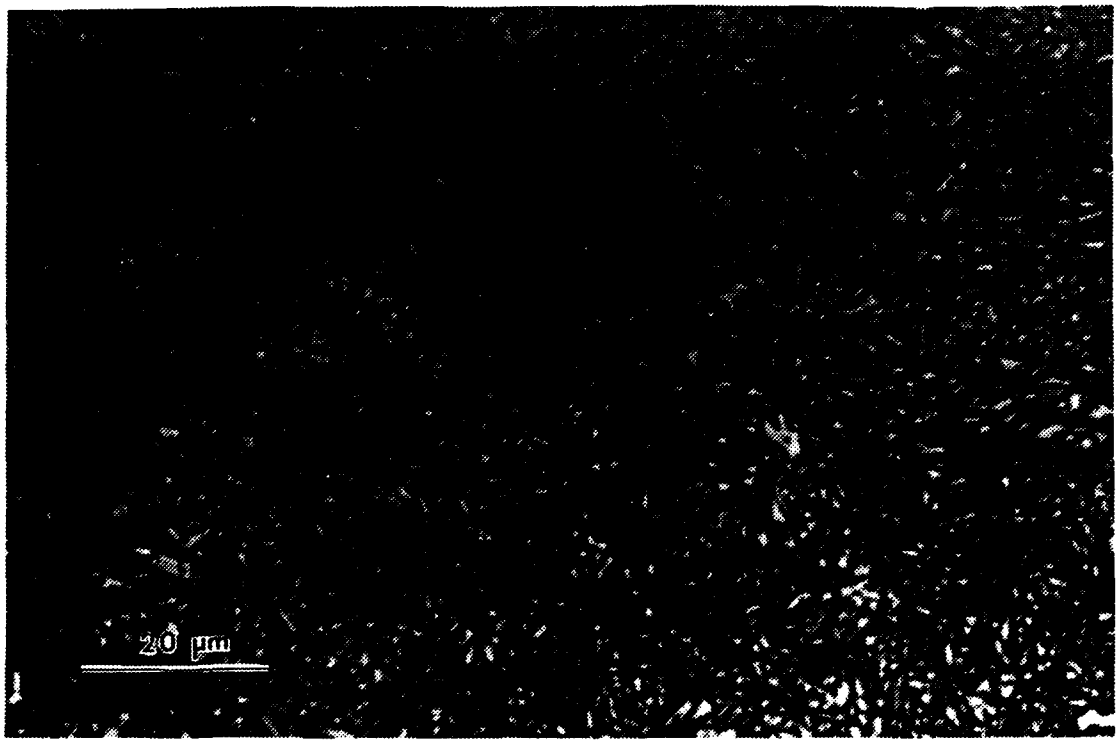

Figure 3.11 Warm-Rolled (700°C), 1106°C (1270X)

microstructure) together. These results indicate that future work in this study should be conducted using austenitizing times of shorter duration, and probably as short as one to two minutes.

Comparing Tables II and III, note also that there is generally only a slight softening in the material (approximately five to eight Rockwell C numbers) with tempering. For the two warm-rolled materials austenitized at 1106°C, there is effectively no softening at all (one-half to one Rockwell number). This result is due to secondary hardening, a precipitation hardening resulting from fine temper carbides which precipitate from solution during the tempering cycle. This reaction is kinetically similar to the hardening which occurs in heat-treatable aluminum alloys, and counters the decrease in hardness which accompanies tempering in low alloy steels. This illustrates the two strengthening mechanisms in high speed tool steels: (1) heating to and quenching from the austenitic region to form a supersaturated, hardened martensitic matrix, and (2) tempering to diffuse carbon and--more importantly--to precipitate temper carbides for secondary hardness [Ref. 15].

C. MICROSCOPY OF HARDENED AND TEMPERED SPECIMENS

In preparation for rolling contact fatigue testing, the specimens were subjected to the temper cycle documented

above in chapter II. Figure 3.12 is a micrograph (1270X) of the as-received material which has been austenitized at 1006°C, while Figure 3.13 shows the same starting material at an identical magnification, hardened at 1106°C. Though not immediately clear from the micrographs, there has been a slight increase in grain size with the higher temperature. Figures 3.14 and 3.15 show the warm-rolled material (700°C) austenitized at 1006 and 1106°C, respectively. Distinct grain size refinement is observed in the warm-rolled material (Figure 3.14) over the as-received condition (Figure 3.12) at the same hardening temperature. Comparing the warm-rolled material at the different temperatures, a marked jump in grain size is noted with the higher austenitizing temperature here as well.

Note that there has been no appreciable refinement in the size of the insoluble, residual carbides from Figures 3.12 and 3.13 (as-received) to Figures 3.14 and 3.15 (warm-rolled); neither do these residual carbides appear to have been "broken up" by the warm-rolling process. Bear in mind that this conclusion has been established by a careful, qualitative scan over the entire specimen surface at each condition, not just through the field of view of one micrograph. At no point in this research, in fact, has there ever been any clear and convincing evidence of insoluble carbide refinement with thermomechanical processing. Their persistence even after heat treatment and warm-rolling lends

Figure 3.12 As-Received Material, 1006°C (1270X)

Figure 3.13 As-Received Material, 1106°C (1270X)

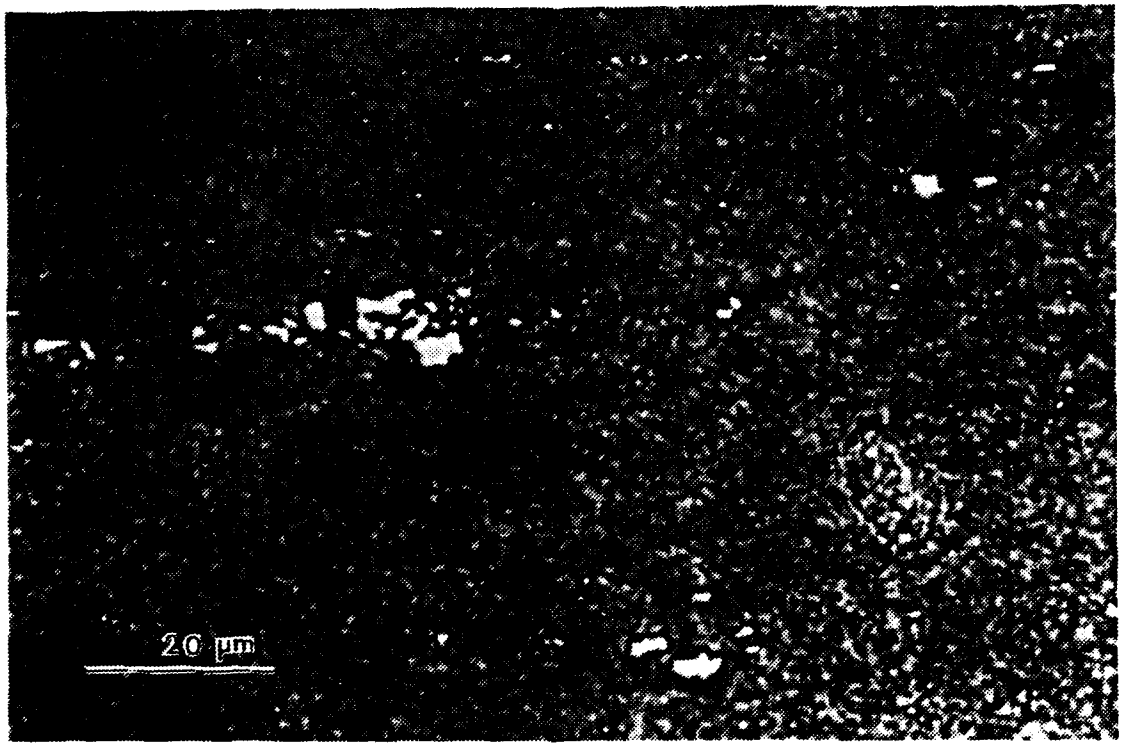

Figure 3.14 Warm-Rolled (700°C), 1006°C (1270X)

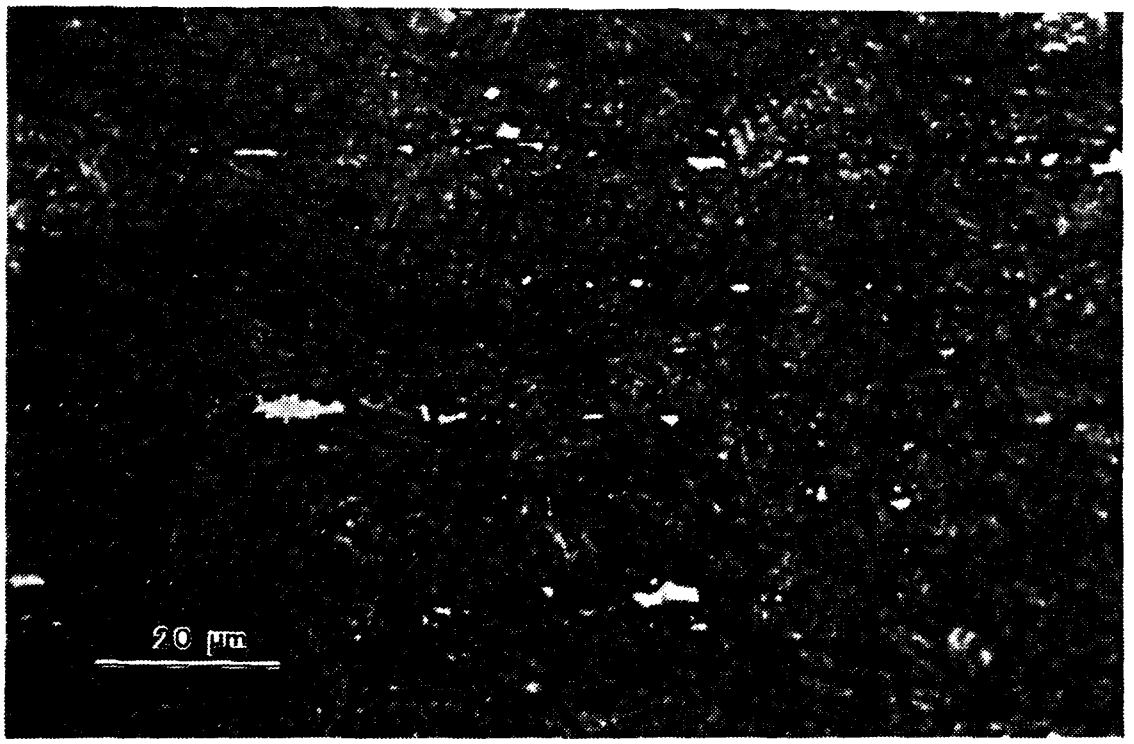

Figure 3.15 Warm-Rolled (700°C), 1106°C (1270X)

support to the belief that their refinement in this steel may not be possible by thermomechanical processing.

Under the scanning electron microscope, the morphologies looked quite similar. Figure 3.16 offers two views of residual carbides taken at the same magnification (6000X) in the as-received material hardened at 1006°C. Note the irregular features of the massive, insoluble carbides and also the cavitation existing at points on their surfaces. Observe also the homogeneous dispersion of the spheroidized temper carbides in the matrix, as well as the fine, randomly-oriented martensite needles which can be clearly resolved at this magnification.

D. ROLLING CONTACT FATIGUE TESTING

As a consequence of longitudinal cracking which occurred during the tempering cycle (detailed below in section F), only four test rods were available for rolling contact evaluation. All four rods tested in rolling contact by NAPC evidenced failure by classical fatigue spalling [Ref. 2]. As an example of this, wear tracks and spalls for the two as-received conditions are shown in Figure 3.17. Spalls varied in length from less than one up to several millimeters, although they were all about 1 mm wide, the thickness of the wear track; fatigue spalls evidenced no characteristic shape. There was no correlation between spall size or shape and the condition being tested; in other words, spalls

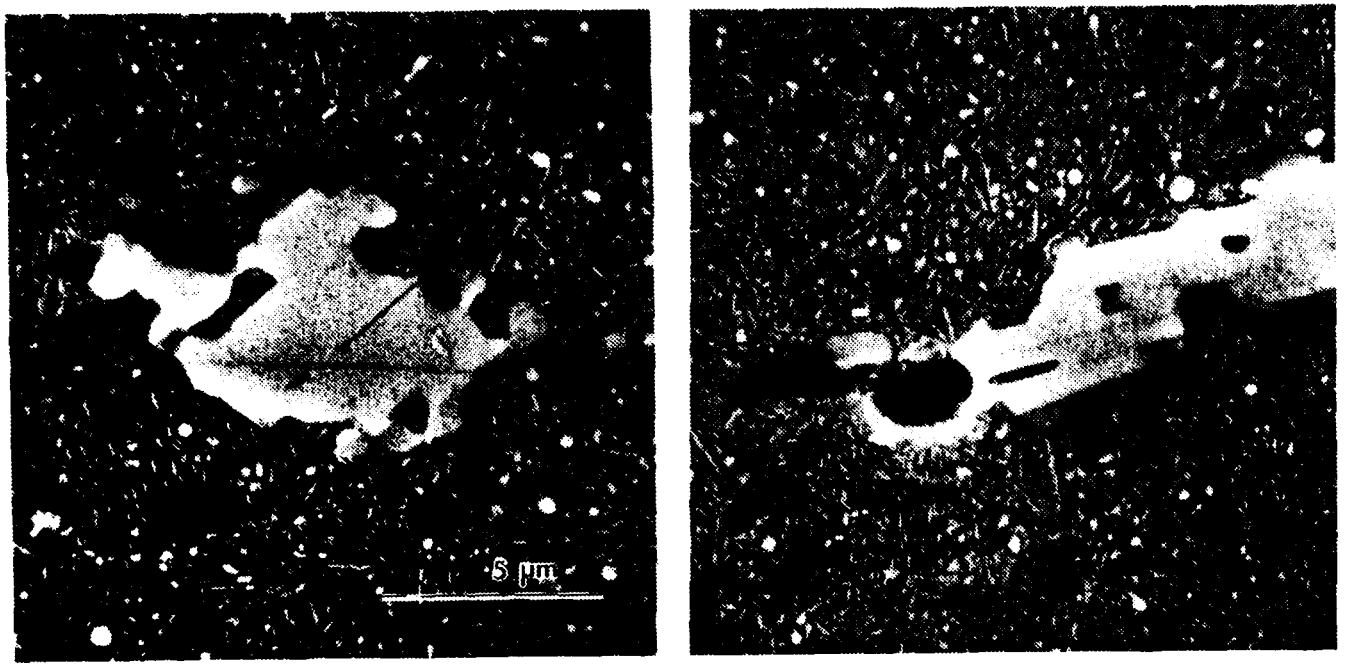

Figure 3.16 As-Received Material, 1006°C (6000X)

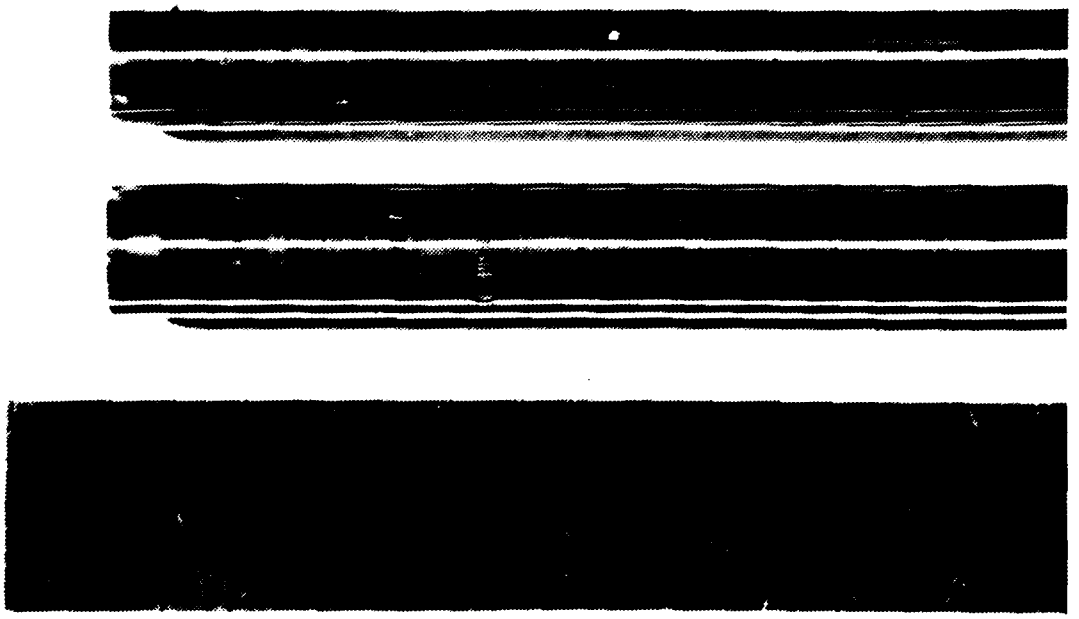

Figure 3.17 Rolling Contact Test Rods, As-Received: 1106°C (Top), 1006°C (Middle)

produced in the as-received material showed no difference in appearance from those occurring on the warm-rolled stock, and vice versa.

The exterior surface of a spall on the as-received material hardened at 1006°C is pictured in Figure 3.18. These two photographs were taken of the same fatigue spall under the scanning electron microscope at a magnification of 90X. In the second micrograph, however, the specimen was tilted at an angle of fifteen degrees relative to its previous position. The result constitutes a "stereo pair," and gives a remarkable three-dimensional effect when seen under a stereo viewer. One is struck by the extent of plastic deformation evident with the spalling action, and by "stretch marks" observed on the surface of the rod showing the direction of the fatigue.

Using optical microscopy, the microstructure below the surface of the spall was examined. The test rods were sectioned longitudinally, so that both the center of the spall and the direction of rolling (evidenced by strings of insoluble carbides) were revealed. Figures 3.19 and 3.20 (406X) depict failures which occurred in the as-received and the warm-rolled (700°C) material, hardened at 1106 and 1006°C, respectively. In neither case was there any obvious interaction between the residual carbides and the cracking which can be observed around the spall, nor was

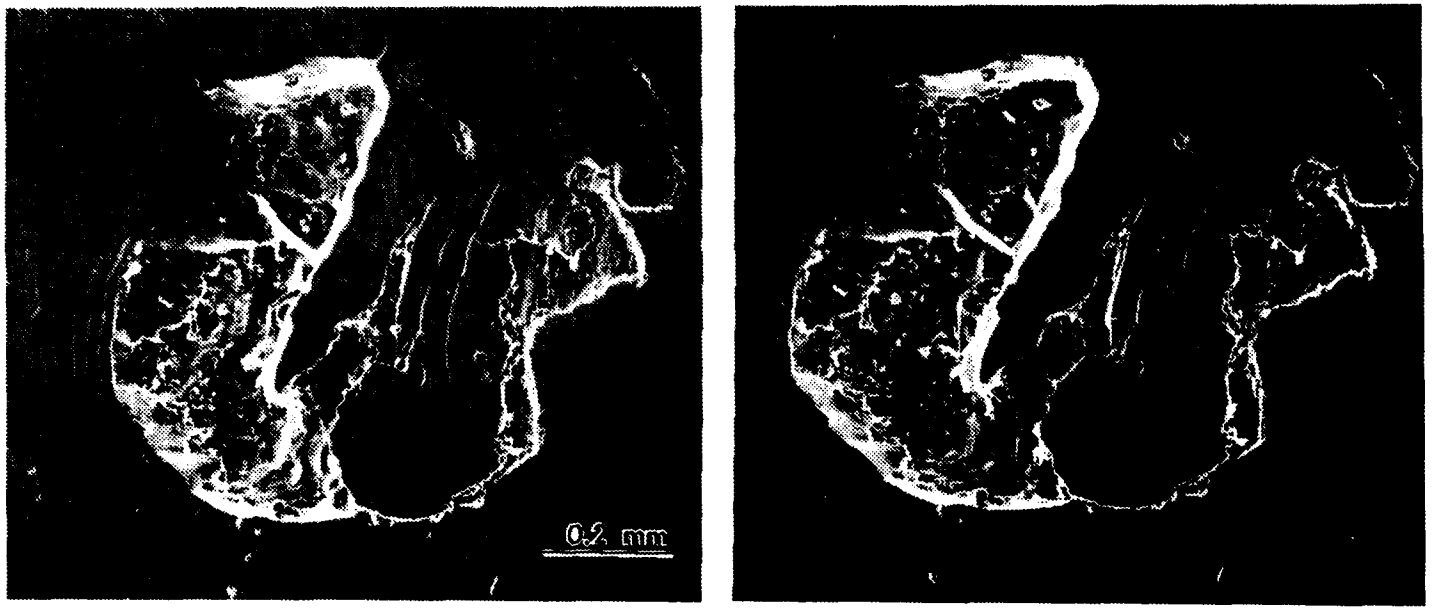

Figure 3.18 "Stereo Pair": As-Received Material, 1006°C (90X)

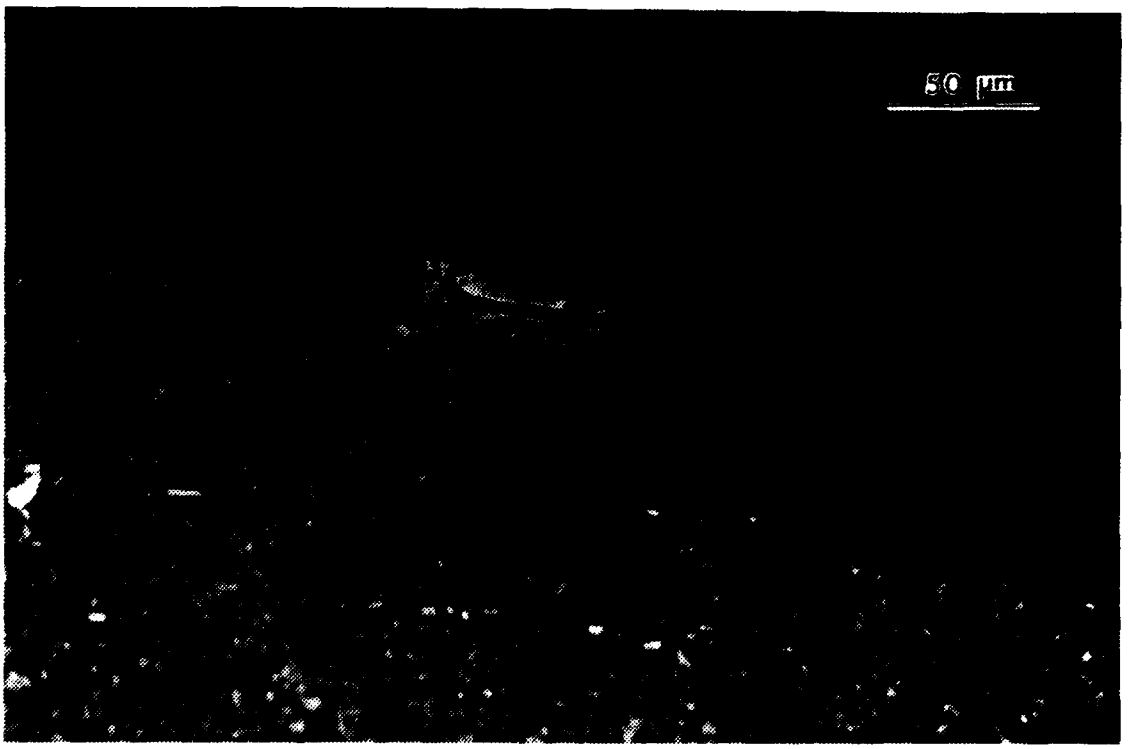

Figure 3.19 Sectioned Fatigue Spall: As-Received Material, Austenitized at 1106°C (406X)

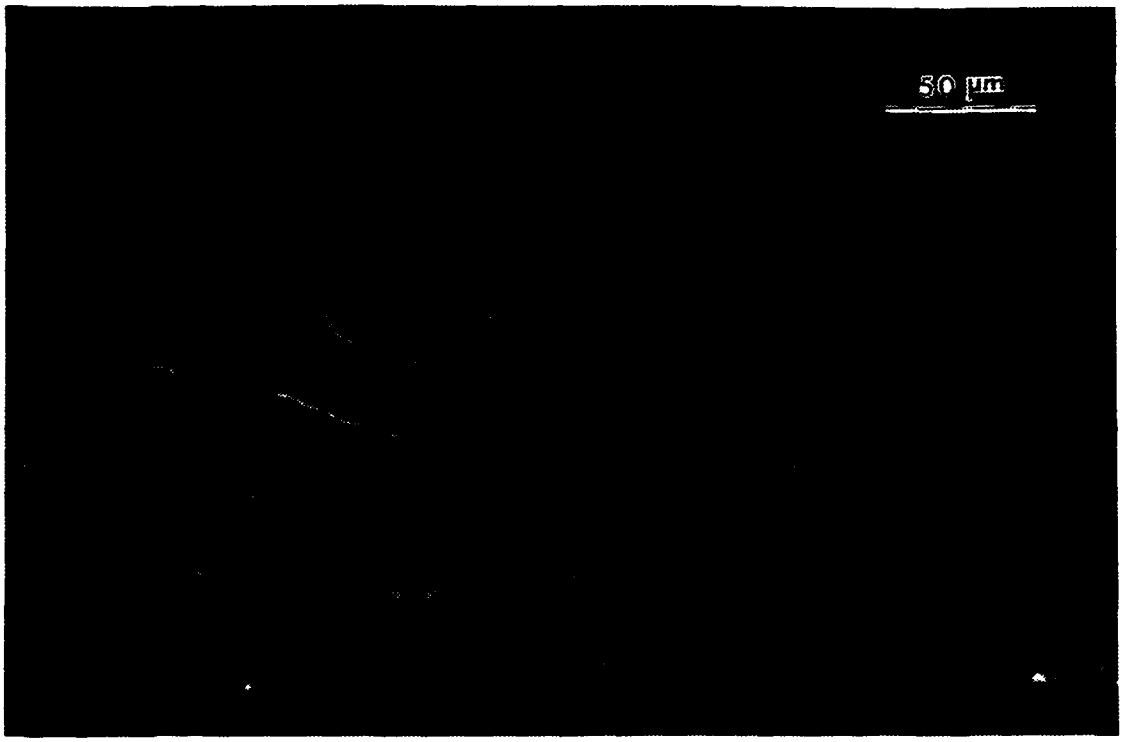

Figure 3.20 Sectioned Fatigue Spall: Warm-Rolled (700°C) Material, Austenitized at 1006°C (406X)

any association seen with the as-received material which had been austenitized at 1106°C (not pictured).

Under the scanning electron microscope, the same specimens were examined again for demonstration of residual carbide interaction. In particular, any apparent coincidence between the insoluble carbides and the start of subsurface cracking (i.e., fatigue spall initiation) was sought. Figure 3.21 reveals a crack on the edge of a spall in the as-received material, austenitized at 1006°C. The micrograph, at 3000X, exhibits carbides which appear to be caught in the path of the crack and were themselves broken up. The corona which outlines the edge of the spall in this photograph is a result of electron charging of the metallographic sample. Observe also that temper carbides can be resolved at this magnification. In Figure 3.22, the apparent origin of another crack in the same material is shown at a higher magnification (6000X). Here, the same phenomenon is seen: that of a fatigue crack originating in the matrix and propagating through a carbide to the surface of the rod, eventually resulting in a spall. Note the fissure pattern in the carbide itself, revealing the direction of crack growth and travel to be from the interior of the specimen to its surface. Again, however, the insoluble carbide appears simply to have been an obstacle, rather than an initiator, for the crack. Another micrograph taken of the same sample, Figure 3.23, shows fatigue-induced cracks

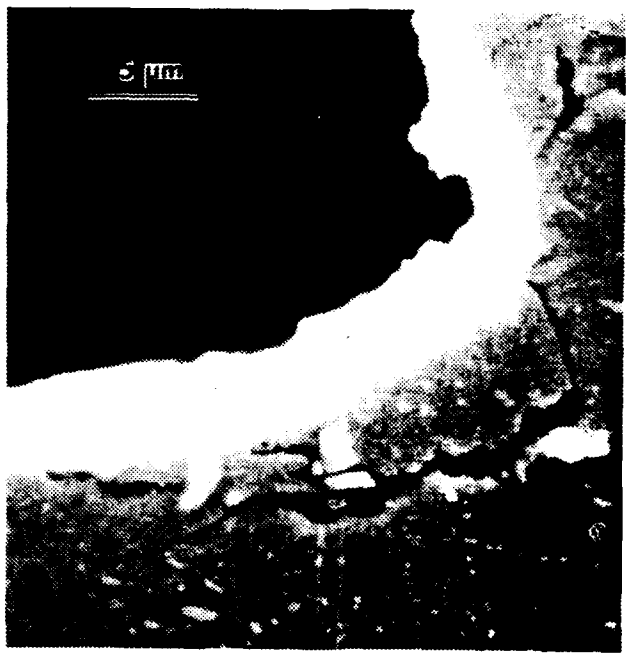

Figure 3.21 Sectioned Fatigue Spall: As-Received Material, Austenitized at 1006°C (3000X)

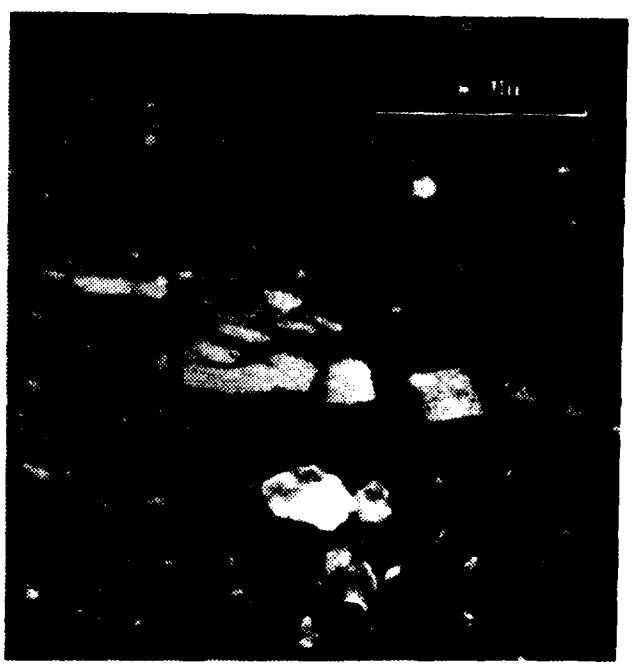

Figure 3.22 Sectioned Fatigue Spall: As-Received Material, Austenitized at 1006°C (6000X)

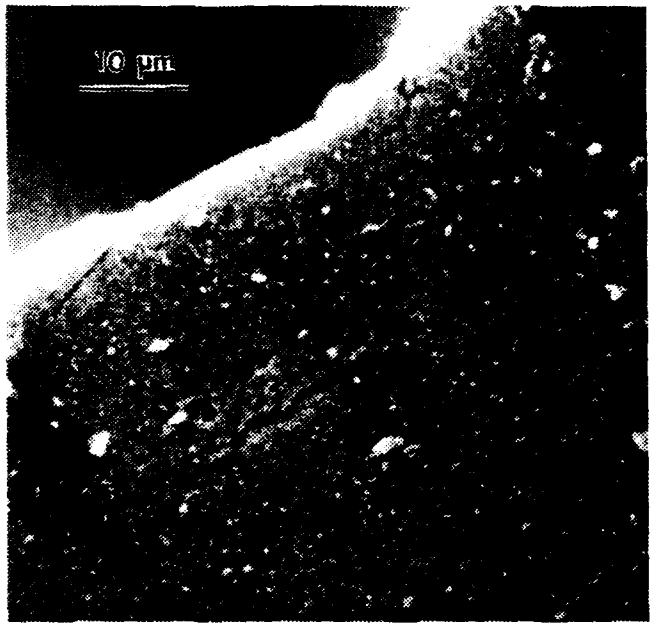

Figure 3.23 Sectioned Fatigue Spall: As-Received Material, Austenitized at 1006°C (1500X)

which have formed immediately beneath the area where the spall eventually occurred. These cracks (shown at 1500X) developed in the matrix amidst a relatively homogeneous dispersion of both residual and temper carbides, but do not appear to have been affected (or determined) by the presence of these carbides. This pattern is exhibited in the other conditions as well. As-received material hardened at 1106°C is shown in Figure 3.24 (3000X), and depicts subsurface cracking in the spall region which is also apparently unaffected by the insoluble carbides.

It must be noted, however, that these cracks do not necessarily represent the main crack front which resulted in the fatigue spall. Instead, they constitute additional, or secondary, cracking which has occurred beneath the spall, the evidence of the main cracking having been carrried away with the metallic remnants which comprised the spall itself. With this fact borne in mind, microscopy of failed M-50 steel specimens still yields no evidence that these secondary cracks have nucleated within the insoluble carbides themselves; neither does this fatigue-induced cracking appear to be initiated or influenced by the presence of the residual carbides within the substructure.

E. WEIBULL ANALYSIS

The plots generated from the Weibull function are shown as Figures 3.25 through 3.28. A complete description of the

Figure 3.24 Sectioned Fatigue Spall: As-Received Material, Austenitized at 1106°C (3000X)

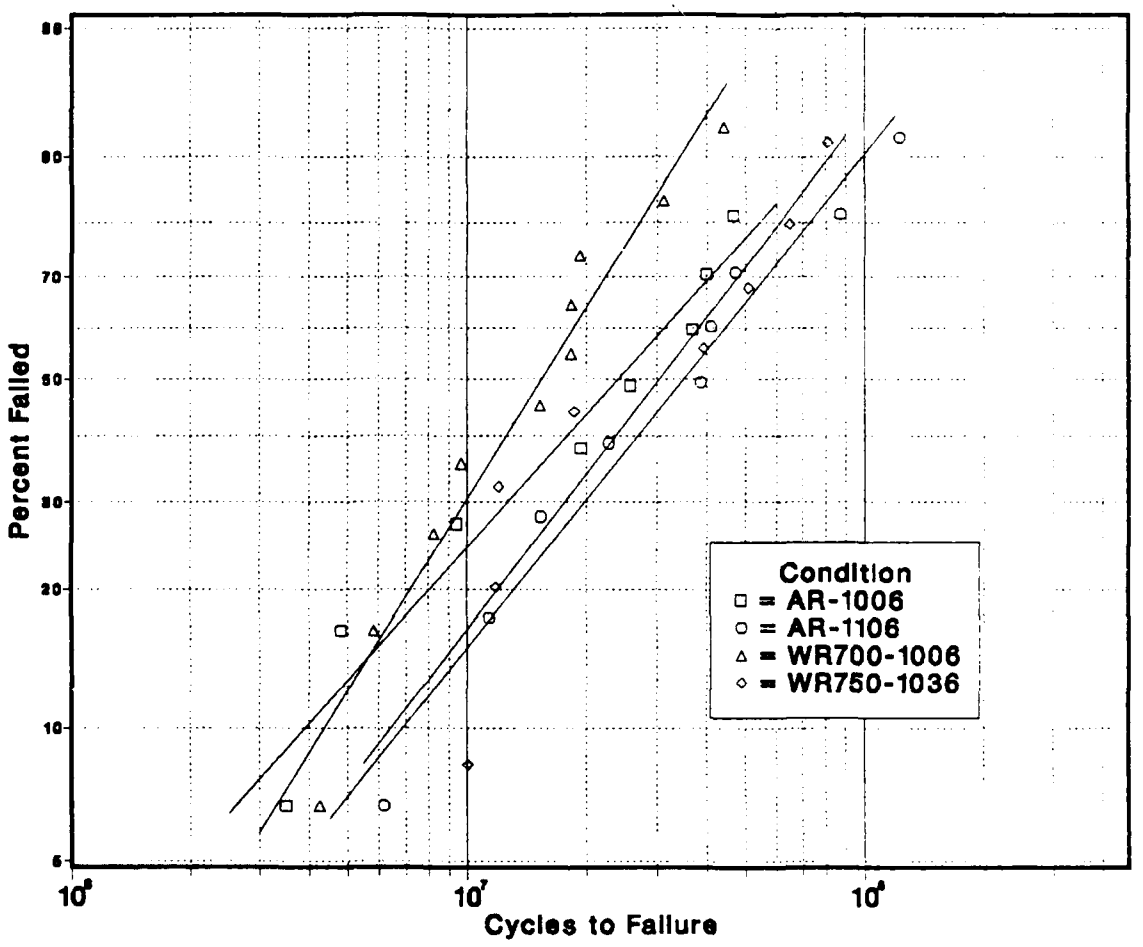

Figure 3.25 Weibull Distribution

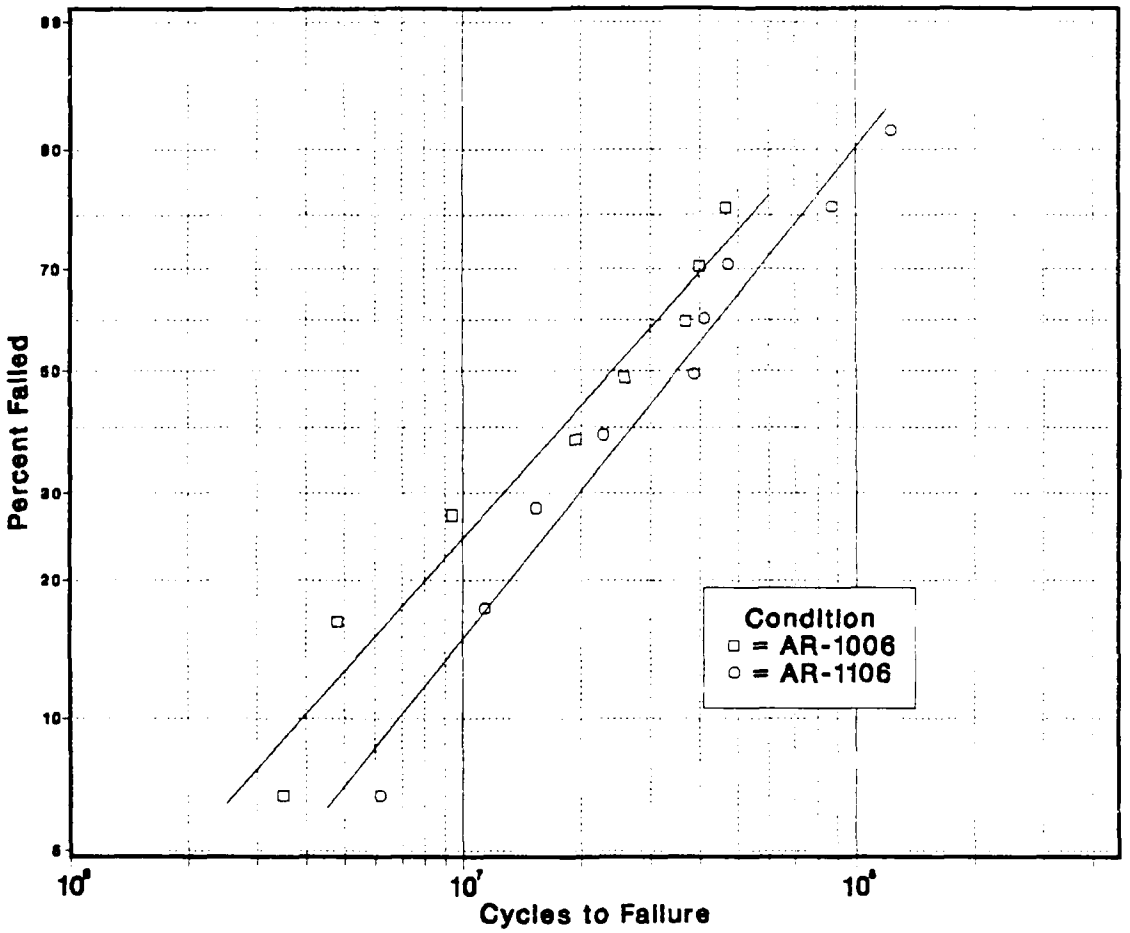

Figure 3.26 Weibull Distribution

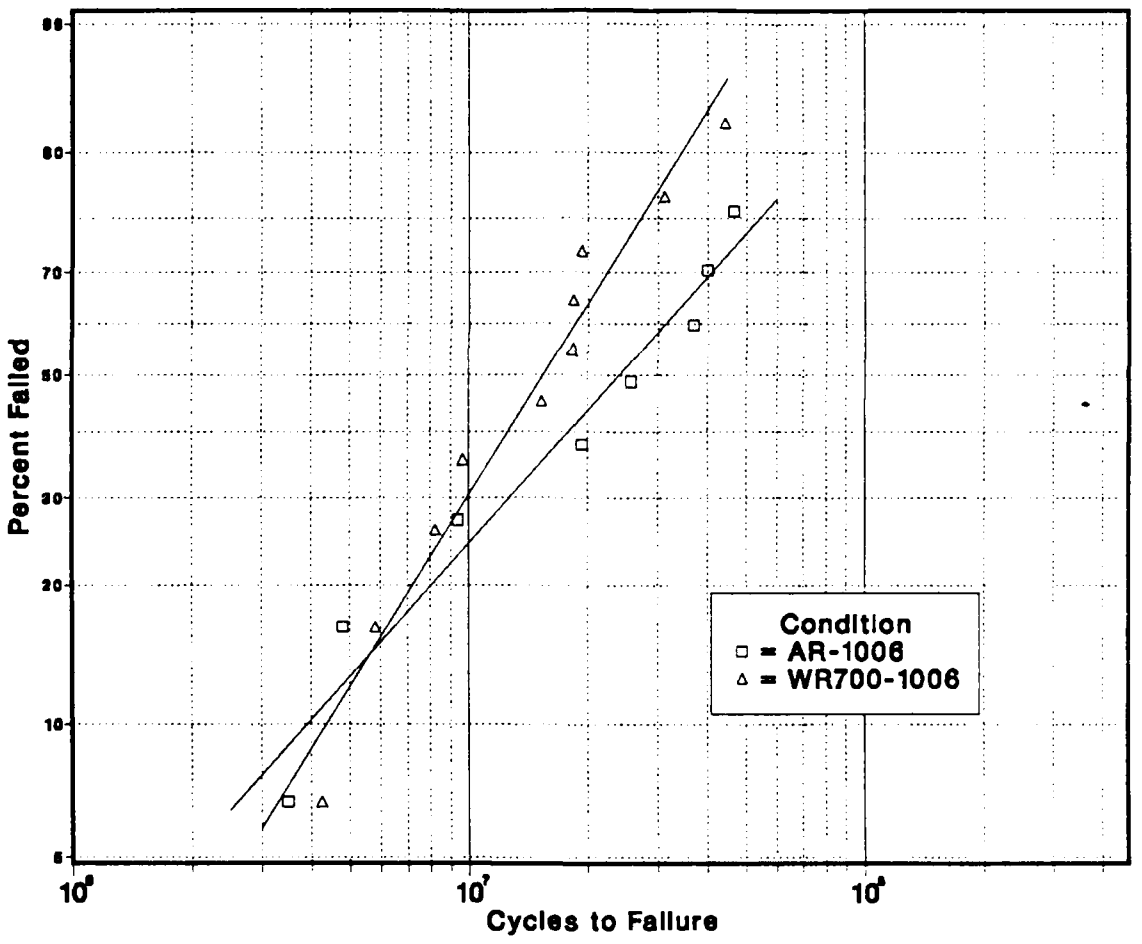

Figure 3.27 Weibull Distribution

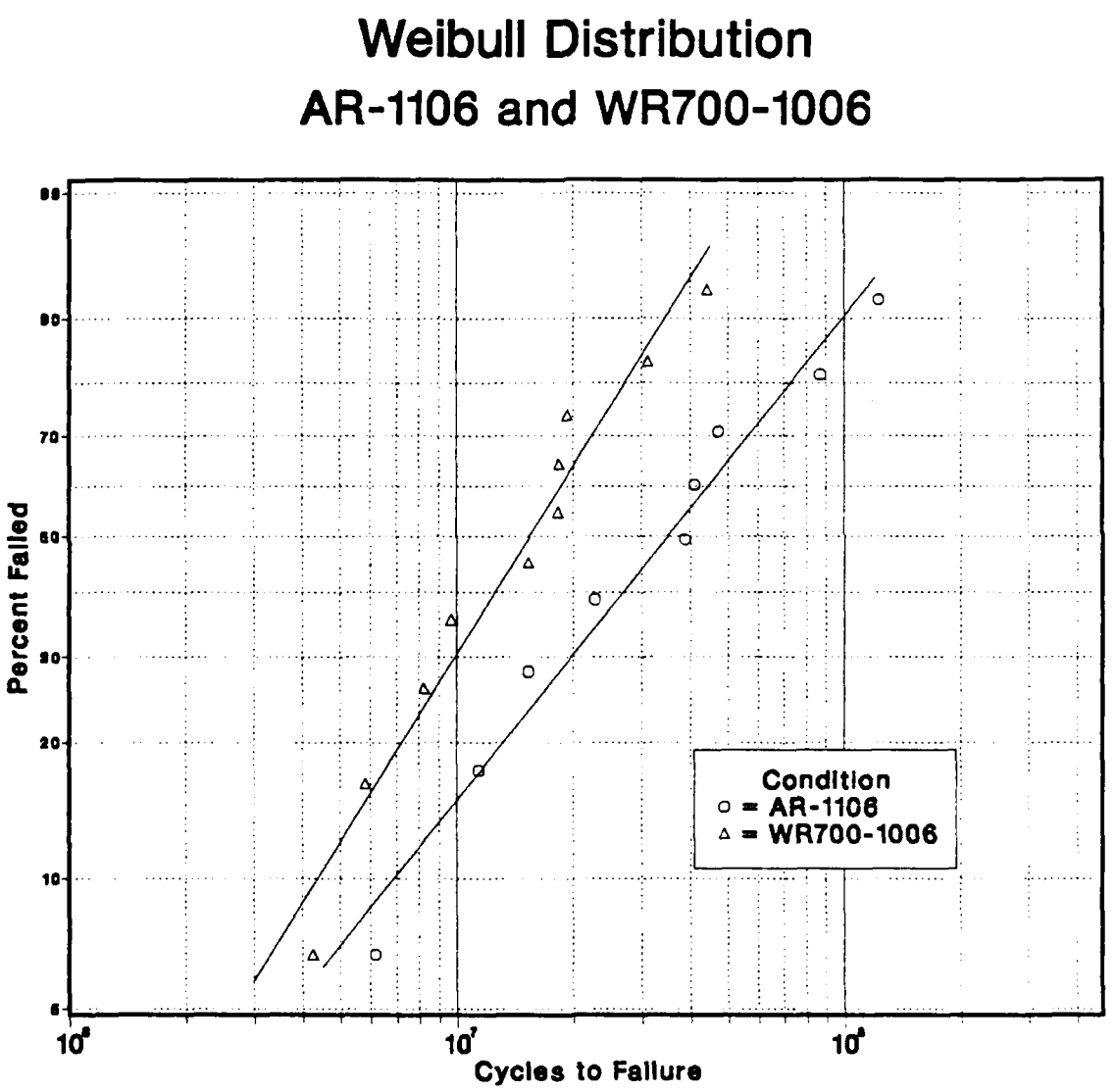

Figure 3.28 Weibull Distribution

Weibull analysis is given by Johnson in Reference 16. The empirical data used to produce these graphs are given in Appendix A, which also includes supplementary calculations such as the Weibull slopes, characteristic lives, and correlation coefficients. The bar codes listed in Appendix A correspond to the following material processing conditions:

A-1 As-received, 1006°C

F-2 As-received, 1106°C

K-3 Warm-rolled (700°C), 1006°C

N-2 Warm-rolled (750°C), 1036°C

For each test rod, discrete points representing the number of cycles to failure and the "median rank" of each failure determination (i.e., a cumulative distribution, from zero to one hundred percent, which indicates how many failures have occurred) were plotted. Then, a linear regression (least squares) analysis was performed, and the resultant "best-fitting" straight line for these points was overlaid on the graph.

Figure 3.25 shows all four test rods/conditions on a Weibull plot. Noteworthy is the fact that there are no vast differences in rolling contact fatigue life among the test conditions. The Weibull slopes for three of four rods are essentially equal, while the slope for the warm-rolled (700°C) material austenitized at 1006°C is inexplicably (and perhaps insignificantly) higher. Allowing for statistical scatter and the relatively small number of tests

run per sample, the results demonstrate virtual equivalence. This is particularly significant (and reasonable) in light of the similarities in microstructure and hardness which have already been documented for this material. Therefore, one must conclude that, for the heat treatments here with a five-minute austenitizing time, there appears to be no dependence of rolling contact fatigue behavior on prior processing history. Further testing in rolling contact fatigue must be conducted on materials which have been heat treated for shorter holding times. As noted previously, this may facilitate determination of the effects of microstructural refinement, assuming such refinement is better retained at the shorter austenitizing times.

However, neither can the effect of voids associated with the insoluble carbides be neglected. It is quite possible that, regardless of the microstructural enhancement gained by thermomechanical processing, cavitation is the controlling feature which determines the fatigue life of rolling elements fabricated from M-50 steel. If these voids act as stress raisers in the matrix, they would have the same propensity to act as sites for crack nucleation in the substructure as porosity or oxide inclusions. This condition effectively nullifies the benefits gained by VIM-VAR processing during manufacture of the steel, accomplished that these impurities might be removed [Ref. 17].

Because the intricacy of Figure 3.25 makes it difficult to read, three additional plots were generated using the same data. Figure 3.26 compares the two as-received conditions. There it is observed that the material heat treated at the higher temperature clearly demonstrates a superior resistance to rolling contact fatigue. The mean life of the as-received material austenitized at 1006°C is 33.66 million cycles (Appendix A), compared with 45.81 million cycles for the same material hardened at 1106°C, an increase in average fatigue life of 36.1 percent. One would predict a greater resistance to rolling contact fatigue for the latter material simply on the basis that, at the higher austenitizing temperature, more carbides are dissolved and hence more carbon is taken into solution, yielding a harder microstructure. In reality, however, Rockwell readings for these materials, found in Table III, show that they are effectively identical in hardness, taking the standard deviation of the readings into account. So, even with an obviously inferior (larger) grain size, the as-received material austenitized at the higher temperature delivers a significantly better response in rolling contact testing.

The results from the as-received and warm-rolled (700°C) test rods, both austenitized at 1006°C, are shown in Figure 3.27. The data are very similar at the lower percentages of failure, but the as-received material outperformed the warm-rolled stock as the testing continued. The mean life

of the warm-rolled material (17.80 million cycles) was 47.1 percent less than the as-received condition (33.6 million cycles). Although one must be careful when attempting to extrapolate conclusions, given the nature of the statistical data and the reasons outlined above, the analysis still points to the fact that at least the warm-rolled material is no better than the as-received condition in terms of rolling contact fatigue performance. And, if carbide size and dispersion are, as has been postulated [Refs. 18-20], the dominant factors (vice mere refinement of the matrix) affecting rolling contact fatigue life, then the Weibull analysis alone--microscopy aside--strongly suggests that the insoluble carbides have not been refined by thermomechanical processing.

Figure 3.28, a comparison of the as-received material hardened at 1106°C and the warm-rolled (700°C) material austenitized at 1006°C, shows the as-received material to be superior to the warm-rolled condition by an approximate factor of two. This serves only to amplify the conclusions of the previous two plots and provides no new information.

F. EFFECTS OF RETAINED AUSTENITE

Rolling contact test specimens which had been warm-rolled and then subjected to the higher hardening temperature (1106°C) experienced longitudinal cracking during the post-austenitizing tempering cycle. This result led to an

investigation into the amount of stable austenite which was retained at room temperature after heat treatment. Subsequently, additional samples were austenitized at "mid-range" temperatures of 1036 and 1066°C, in order to determine if a critical temperature could be established, beyond which no more cracking occurred. These test rods were examined carefully after hardening and found to be free from surface cracks. After the first tempering cycle (i.e., two hours of freezing followed by two hours of tempering), however, all samples exhibited longitudinal cracking as before.

These cracks generally traversed the entire axial length of the test rod (about four inches) and penetrated to a range of depths, from less than 1 mm below the surface to the entire 0.375 inch (9.5 mm) diameter of the rod. An example of this extensive cracking is shown in Figure 3.29, which exhibits a sample of the warm-rolled (750°C) material, austenitized at 1066°C, mounted in phenolic compound and polished.

At first it was assumed that these cracks were the result of too rapid a quench from the austenitizing temperature. This idea of severity of quench was discarded, however, when further thought was given to the actual heat treatment (i.e., stabilization of the test rod in molten salt following austenitization, then air cooling to room temperature), which gave sufficient time for residual stresses to be accommodated in the material. Instead, it was

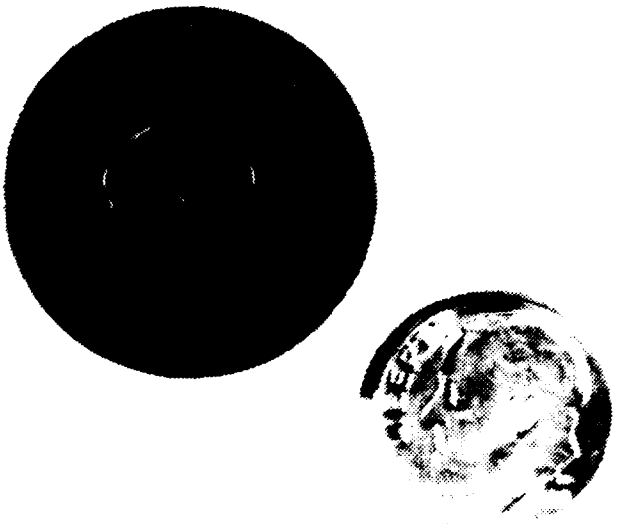

Figure 3.29 Longitudinal Cracking (Cross-Section): Warm-Rolled (750°C) Material, Austenitized at 1066°C

reasoned that the cracking must have resulted from the tempering treatment which followed hardening. Specifically, it was thought to occur during the first freezing cycle, when it was suggested that large quantities of retained austenite transformed to untempered martensite. This would be accompanied by an unfavorable volume change due to the lattice transformation from a face-centered cubic (FCC) crystal structure to a body-centered tetragonal (BCT) structure, which in turn would lead to cracking.

This hypothesis was confirmed by optical microscopy. Figure 3.30 (the same specimen shown in Figure 3.29), shown at a magnification of 1016X, depicts the intersection of a crack with the surface of the test rod. A shallow decarburized layer can be seen at the rod surface, a common defect which occurs during austenitizing (final grinding removes this layer before commencing the rolling contact fatigue test). Decarburization is not evident in the crack, however, indicating that the fissure had not yet been opened during hardening. This result confirms the post-austenitization examination of the rolling contact specimens which found them to be crack-free. Figure 3.30 also reveals that both the rod surface and the crack interior show evidence of oxidation, such as would occur upon tempering. Thus, one concludes that cracking took place after austenitizing but before tempering: i.e., during the deep-freeze phase of treatment.

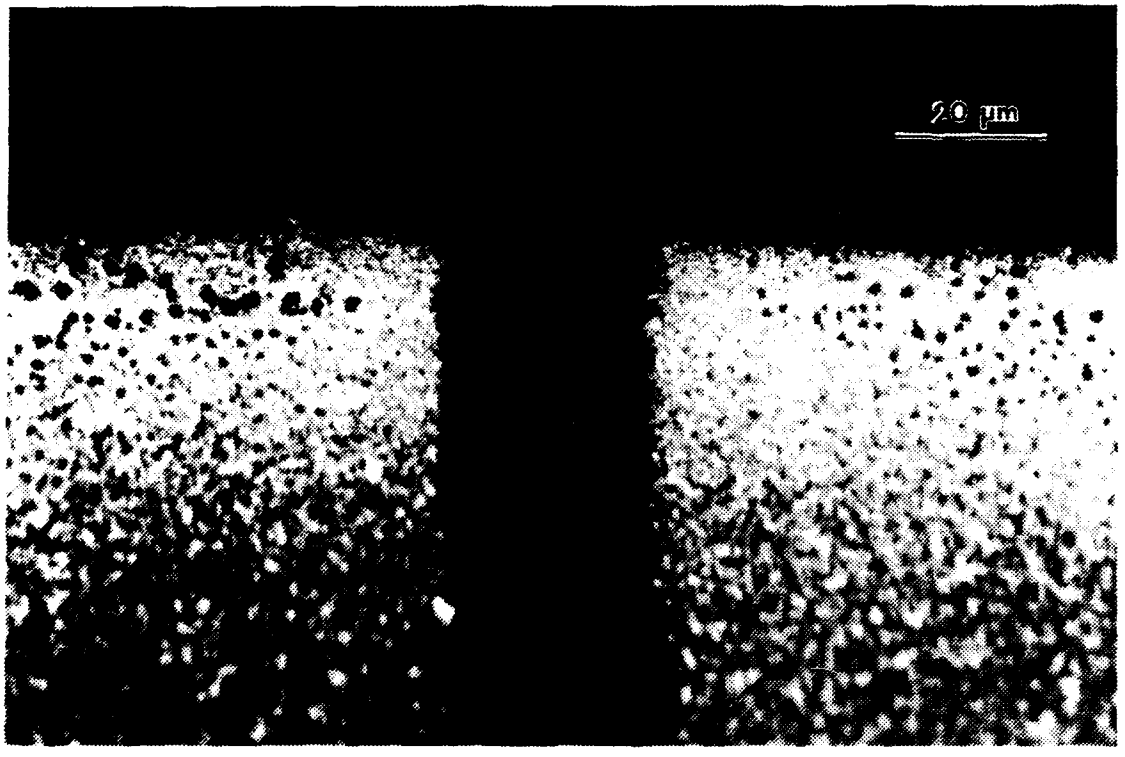

Figure 3.30 Warm-Rolled (750°C) Material, Austenitized at 1066°C (1016X)

Retained austenite has been documented in the metallurgical literature as having a deleterious effect upon rolling contact fatigue life [Refs. 21 and 22]. Apart from austenite being a softer phase than martensite, there is always the danger that stresses generated in-service can activate a transformation to martensite. This will lead to volume and possibly shape changes (due to the change in lattice structure). Also, the presence of a local residual stresses could also assist in the initiation of fatigue cracking, decreasing the life of the component [Ref. 22].

Complete elimination of retained austenite is not possible, but a combination of freezing and tempering should reduce it to an acceptable minimum in the material [Ref. 22]. The deep-freeze, of course, brings the metal below the martensite finish temperature, which has been lowered due to extensive alloying (such as in M-50 steel), and induces the martensitic transformation. Although the standard heat treatment of austenitized M-50 steel includes these deep-freezing and tempering cycles, recent discussions with a bearings metallurgist indicates that the trend in the industry is now away from the freezing phase, presumably because of the harsh thermal gradients this procedure imposes on a material. Instead, a heat treatment scheme which consists of austenitization followed by multiple tempers is currently being employed [Ref. 23]. Tempering alone at an elevated (though sub-critical) temperature will

also result in the reduction of retained austenite. As carbon diffuses from its interstitial location in the BCT (martensitic) crystal structure, it acts as a ferrite stabilizer, raising the martensite start and finish temperatures; this enables the retained austenite to more completely transform to martensite at a higher temperature.

To qualitatively investigate the presence of retained austenite in the hardened steel, twelve new specimens, all of them approximately one inch (25.4 mm) long and 0.375 inches (9.5 mm) in diameter, were prepared. Each of the three materials (the as-received stock and the two warm-rolled conditions) was subjected to four different austenitizing temperatures: 1006, 1036, 1066, and 1106°C. Samples were left in the as-hardened state (i.e., no tempering treatment was applied). From this experiment, a marked increase in the amount of retained austenite with increasing austenitizing temperature was observed. Compare Figure 3.8 to Figure 3.9 (as-received) and 3.10 to 3.11 (warm-rolled at 700°C) to see the higher retained austenite content resulting from a heat treatment temperature increase from 1006 to 1106°C, respectively. This is evidenced by the numerous white patches of retained austenite which are exhibited throughout the matrix in Figures 3.9 and 3.11, and is due to the greater amount of carbon (from soluble carbides) taken into solution as hardening temperature is raised. Since the solvus of the most tenacious soluble

carbide is just below 1100°C, one would not expect to see a still further increase in the amount of retained austenite with elevated austenitizing temperatures.

As could be anticipated, the degree of cracking was most severe at the higher austenitizing temperatures; this was a result of more carbon being driven into solution, which therefore led to more retained austenite. Cracking existed in the rolling contact test rods themselves only in the warm-rolled material, and was--as expected--more extensive in those specimens austenitized at 1106 and 1066°C, although the rods hardened at 1036°C also exhibited somewhat shallow axial cracking. In the shorter specimens prepared for the retained austenite investigation, however, cracking occurred in all three conditions only at the highest (1106°C) austenitizing temperature, and also in the as-received material hardened at 1066°C. This latter phenomenon, in light of the previous result in the test rods, defies explanation at present.

Since this investigation was merely qualitative in nature, and rather superficial at that, no assessment was made of the actual percentage of stable austenite which was retained in the material following the hardening heat treatment. It will be an important aspect of future reseach in this area to determine, using quantitative x-ray diffraction methods, the amount of retained austenite which remains following the various austenitizations, both before and

after the tempering cycle, so as to gain a clear understanding of its impact on rolling contact fatigue life.

Under the optical microscope, the crack propagation path through the steel was studied. It is noted in passing that the cracks appeared to traverse transgranularly across the specimens. Figure 3.31, however, which shows warm-rolled material (700°C) austenitized at 1106°C (magnification: 813X), reveals in intergranular propagation path. Using scanning electron microscopy at a magnification of 440X, the fracture surface itself (Figure 3.32) exhibits an appearance reminiscent of grain boundary facets ("rock candy"). Although there is a fairly uniform overlay of oxidation products, the surface displays a pattern of rounded, small angle tilts and no clear evidence of plastic deformation, and is thus characteristic of brittle intergranular fracture [Ref. 24].

Figure 3.31 Intergranular Cracking: Warm-Rolled (700°C) Material, Austenitized at 1106°C (813X)

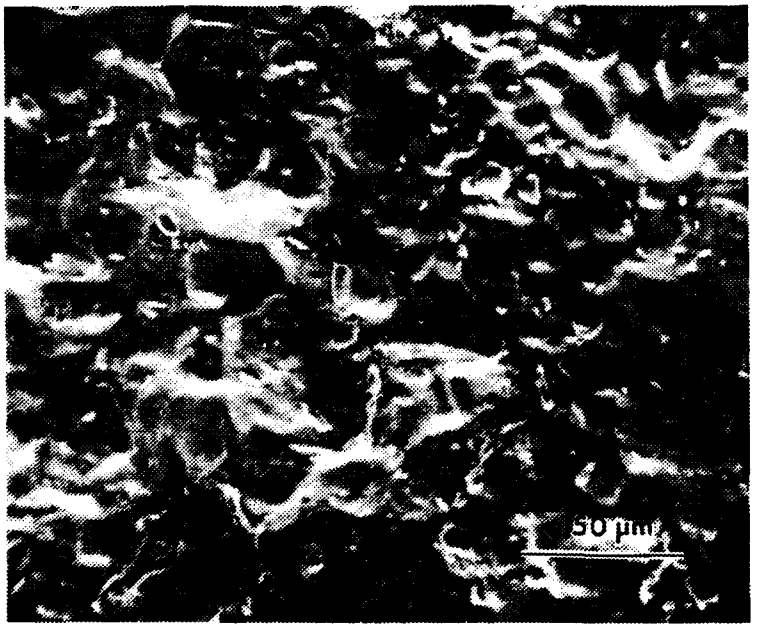

Figure 3.32 Fracture Surface of Warm-Rolled (700°C) Material, Austenitized at 1106°C (440X)

IV. COMMENTARY AND CONCLUSIONS

Thermomechanical processing of M-50 steel has been effective in two areas: (1) refinement of the matrix ferrite grain size in the microstructure, and (2) yielding a fine, homogeneous dispersion of soluble (temper) carbides in that matrix. It has failed to refine, except to a minor extent, the insoluble (residual) carbides MC and M_2C. It has previously been stated that the dominant factor in enhancement of rolling contact fatigue life is believed to be the effect of carbide size and dispersion [Refs. 18-20]. There is sufficient evidence in the literature to adequately support this conclusion.

First, rolling contact fatigue testing performed on carbide-refined AISI 52100 steel showed that fatigue life improvements on the order of a factor of three have been achieved [Ref. 25]. Recall that this is a steel for which all of the carbides may be driven into solution, resulting in a fine-scale, homogeneous matrix. Secondly, the effect of ausforming on M-50 steel has substantially improved the fatigue lives of balls and bearings in rolling contact [Refs. 26 and 27]. With this technique, a uniform dispersion of small carbides is achieved, thereby lessening the severity of dislocation pile-ups which act as stress concentrators and, ergo, sites for crack nucleation. Although

one may justifiably call into question the degree of refinement of the insoluble carbides attained by this method, as documented in Reference 26, the fact remains that there is convincing association between residual carbide refinement and an increase in effective bearing life. Third, it has been shown that a crystallized glass ceramic approximates to a very high degree the properties of a carbide-refined bearing steel, in that the ceramic has very small crystals which are both evenly dispersed and randomly oriented within a matrix, in a manner analogous to the carbides in M-50 steel [Refs. 28 and 29]. This ceramic material exhibited longer fatigue life when the crystals were smaller and more closely spaced. The researcher proposed two reasons why this occurred: (1) the crystals (or carbides in a bearing steel) would tend to block the formation of longer cracks by acting as an inhibitor to crack propagation, and (2) the crystals or carbides would strengthen the area of resolved shearing stress more if they were close together than if they were widely separated, thus retarding crack initiation [Ref. 28].

The preceeding discussion all suggests that the thermomechanical processing employed here is unable to refine the insoluble carbides and may therefore be of no use in gaining an enhancement of rolling contact fatigue resistance in M-50 steel. There are two critical experiments necessary to confirm this, however. First, shorter austenitizing times

must be investigated, to see if matrix refinement produced by thermomechanical processing can be retained during austenitization and effect an enhancement of rolling contact fatigue life. Second, an experiment should be structured which removes (closes up) the voids present in these materials. A method such as hot isostatic pressing (HIP), used in processing of powder metallurgy, or another appropriate technique could be employed for this purpose. This would determine the extent to which the cavitation is relevant to the rolling contact fatigue behavior of this steel.

The conclusions relating to this research into the rolling contact fatigue life of thermomechanically processed M-50 steel are summarized as follows:

1. Thermomechanical processing has resulted in the significant refinement of both the ferrite grain size and the soluble (temper) carbides.
2. Thermomechanical processing has failed to yield any more than a minor refinement of the insoluble (residual) carbides, which occur as MC and M_2C in M-50 steel.
3. The hardness of all specimens hardened with a five-minute holding time is fundamentally constant, with only a slight softening observed at the highest austenitizing temperature.

4. The five-minute austenitization time is too long for the small size of the test materials used, and results in an undesirable homogenization with respect to both microstructure and hardness.
5. There was no correlation between surface fatigue spall size or shape and the heat treatment condition under evaluation.
6. Optical and scanning electron microscopy of failed specimens yields no evidence that secondary stress cracking has nucleated within the insoluble carbides; neither does fatigue-induced cracking appear to be initiated or influenced by the presence of residual carbides in the substructure. Evidence of such interaction, however, is strongly alluded to in the literature.
7. Weibull analysis demonstrates the essential equivalence of the results of the rolling contact fatigue testing. With a five-minute austenitizing time, there appears to be no dependence of rolling contact fatigue behavior on prior processing history.
8. The thermomechanically processed material is not better than the as-received condition in terms of rolling contact fatigue performance.
9. Longitudinal cracks occurring the specimens following austenitization are the result of excessive retained austenite which transforms to

untempered martensite during the deep-freeze phase of the tempering cycle.

10. The extent of axial cracking is more severe at the higher austenitizing temperatures. This is due to the fact that more carbon is being taken into solution with the elevated temperature, which in turn results in greater quantities of retained austenite.

V. RECOMMENDATIONS FOR FUTURE WORK

The following recommendations constitute additional research opportunities in this area:

1. Conduct rolling contact fatigue testing on specimens subjected to different thermomechanical processing conditions and austenitized at hardening holding times of less than five minutes.
2. Remove existing cavitation through hot isostatic pressing (HIP) and test these specimens in rolling-element fatigue.
3. Determine quantitatively, using x-ray diffraction methods, the amount of retained austenite which remains following heat treatment at various austenitizing temperatures.
4. Investigate exhaustively the relationship between insoluble carbides in the substructure and the initiation of interior stress cracking which leads to failure by fatigue spalling

Naval Air Propulsion Center
Trenton, N.J.

Weibull Statistical Analysis
of Rolling Contact Fatigue Data

R.C.F. Evaluation of Thermo-Mechanically Processed M-50
Bar Code: A-1

Number of Specimens Tested = 10 Number Failed = 8 A-1

Order No.	Median Rank	Failed Specimens (Millions of Cycles)	X Value	Y Value
1.0000	0.06697	3.49	0.124990E+01	-2.669099
2.0000	0.16320	4.80	0.156862E+01	-1.725039
3.1250	0.27145	9.37	0.223751E+01	-1.149783
4.2500	0.37971	19.31	0.296062E+01	-0.739038
5.3750	0.48797	25.74	0.324805E+01	-0.401411
6.5000	0.59623	36.90	0.360821E+01	-0.097713
7.6250	0.70449	39.90	0.368638E+01	0.198068
8.7500	0.81275	46.51	0.383967E+01	0.515986

Specimen life values with 90 Percent Confidence Bands

	Lower Band	Upper Band
L(10)LIFE = 3.90	0.87	34.16
L(50)LIFE = 23.99	12.14	47.48

Weibull Slope = 1.0373
Correlation Coefficient = 0.85641
Characteristic Life = 34.42

Mean Life = 33.66
F(X) = 0.63

X-Mean = 0.279987E+01
Standard Deviation of X = 0.998700E+00
Stan. Dev. of X--Squared= 0.997403E+00

Naval Air Propulsion Center
Trenton, N.J.

Weibull Statistical Analysis
of Rolling Contact Fatigue Data

R.C.F. Evaluation of Thermo-Mechanically Processed M-50
Bar Code: A-1

Number of Specimens Tested = 10 Number Failed = 8 A-1

Life of Specimen (Millions of Cycles)	Failure Code
3.49	F
4.80	F
7.92	D
9.37	F
19.31	F
25.74	F
36.90	F
39.90	F
46.51	F
117.80	D

(F=Failed; D=Discontinued)

Naval Air Propulsion Center
Trenton, N.J.

Weibull Statistical Analysis
of Rolling Contact Fatigue Data

R.C.F. Evaluation of Thermo-Mechanically Processed M-50
Bar Code: F-2

Number of Specimens Tested = 10 Number Failed = 9 F-2

Order No.	Median Rank	Failed Specimens (Millions of Cycles)	X Value	Y Value
1.0000	0.06697	6.16	0.181808E+01	-2.669099
2.1111	0.17389	11.34	0.242834E+01	-1.655347
3.2222	0.28081	15.30	0.272785E+01	-1.109783
4.3333	0.38773	22.72	0.312325E+01	-0.712156
5.4444	0.49465	38.70	0.365584E+01	-0.381975
6.5556	0.60158	41.08	0.371552E+01	-0.083123
7.6667	0.70850	47.25	0.385545E+01	0.209212
8.7778	0.81542	86.90	0.446476E+01	0.524532
9.8889	0.92234	122.74	0.481007E+01	0.938219

Specimen Life Values with 90 Percent Confidence Bands

		Lower Band	Upper Band
L(10)LIFE =	6.87	1.79	48.19
L(50)LIFE =	35.09	19.02	64.76

Weibull Slope	= 1.1549	F(X)	= 0.61
Correlation Coefficient	= 0.87656	X-Mean	= 0.339991E+01
Characteristic Life	= 48.52	Standard Deviation of X	= 0.966271E+00
Mean Life	= 45.81	Stan. Dev. of X--Squared	= 0.933679E+00

Naval Air Propulsion Center
Trenton, N.J.

Weibull Statistical Analysis
of Rolling Contact Fatigue Data

R.C.F. Evaluation of Thermo-Mechanically Processed M-50
Bar Code: F-2

Number of Specimens Tested = 10 Number Failed = 9 F-2

Life of Specimen (Millions of Cycles)	Failure Code
6.16	F
10.35	D
11.34	F
15.30	F
22.72	F
38.70	F
41.08	F
47.25	F
86.90	F
122.74	F

(F=Failed; D=Discontinued)

Naval Air Propulsion Center
Trenton, N.J.

Weibull Statistical Analysis
of Rolling Contact Fatigue Data

R.C.F. Evaluation of Thermo-Mechanically Processed M-50
Bar Code: K-3

Number of Specimens Tested = 10 Number Failed = 10 K-3

Order No.	Median Rank	Failed Specimens (Millions of Cycles)	X Value	Y Value
1.0000	0.06697	4.25	0.144692E+01	-2.669099
2.0000	0.16320	5.80	0.175786E+01	-1.725039
3.0000	0.25943	8.22	0.210657E+01	-1.202874
4.0000	0.35566	9.67	0.226903E+01	-0.822067
5.0000	0.45189	15.26	0.272523E+01	-0.508710
6.0000	0.54811	18.27	0.290526E+01	-0.230260
7.0000	0.64434	18.33	0.290854E+01	0.033234
8.0000	0.74057	19.23	0.295647E+01	0.299574
9.0000	0.83680	31.15	0.343881E+01	0.594873
10.0000	0.93303	44.32	0.379144E+01	0.994568

Specimen Life Values with 90 Percent Confidence Bands

		Lower Band	Upper Band
L(10)LIFE =	4.37	1.54	19.71
L(50)LIFE =	15.42	9.61	24.77

Weibull Slope	= 1.4934	F(X)	= 0.58
Correlation Coefficient	= 0.88222	X-Mean	= 0.263061E+01
Characteristic Life	= 19.82	Standard Deviation of X	= 0.733083E+00
Mean Life	= 17.80	Stan. Dev. of X--Squared	= 0.537411E+00

Naval Air Propulsion Center
Trenton, N.J.

Weibull Statistical Analysis
of Rolling Contact Fatigue Data

R.C.F. Evaluation of Thermo-Mechanically Processed M-50
Bar Code: K-3

Number of Specimens Tested = 10 Number Failed = 10 K-3

Life of Specimen (Millions of Cycles)	Failure Code
4.25	F
5.80	F
8.22	F
9.67	F
15.26	F
18.27	F
18.33	F
19.23	F
31.15	F
44.32	F

(F=Failed; D=Discontinued)

AD-A153 640 ROLLING CONTACT FATIGUE TESTING OF THERMOMECHANICALLY PROCESSED M-50 STEEL(U) NAVAL POSTGRADUATE SCHOOL MONTEREY CA F A BUTTERFIELD DEC 84 2/2

UNCLASSIFIED F/G 20/11 NL

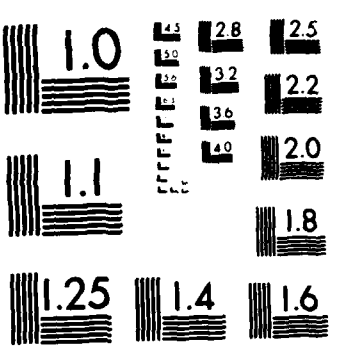

MICROCOPY RESOLUTION TEST CHART
NATIONAL BUREAU OF STANDARDS-1963-A

Naval Air Propulsion Center
Trenton, N.J.

Weibull Statistical Analysis
of Rolling Contact Fatigue Data

R.C.F. Evaluation of Thermo-Mechanically Processed M-50
Bar Code: N-2

Number of Specimens Tested = 8 Number Failed = 8 N-2

Order No.	Median Rank	Failed Specimens (Millions of Cycles)	X Value	Y Value
1.0000	0.08300	10.02	0.230458E+01	-2.445954
2.0000	0.20214	11.82	0.246979E+01	-1.488008
3.0000	0.32128	11.99	0.248407E+01	-0.947904
4.0000	0.44043	18.58	0.292209E+01	-0.543722
5.0000	0.55957	39.34	0.367224E+01	-0.198441
6.0000	0.67872	51.01	0.393202E+01	0.127011
7.0000	0.79786	64.63	0.416868E+01	0.469250
8.0000	0.91700	81.09	0.439556E+01	0.911866

Specimen Life Values with 90 Percent Confidence Bands

		Lower Band	Upper Band
L(10)LIFE =	6.43	1.55	41.19
L(50)LIFE =	30.44	16.29	56.85

Weibull Slope	= 1.2117	F(X)	= 0.60
Correlation Coefficient	= 0.81741	X-Mean	= 0.329363E+01
Characteristic Life	= 41.46	Standard Deviation of X	= 0.843564E+00
Mean Life	= 38.65	Stan. Dev. of X--Squared	= 0.711600E+00

Naval Air Propulsion Center
Trenton, N.J.

Weibull Statistical Canalysis
of Rolling Contact Fatigue Data

R.C.F. Evaluation of Thermo-Mechanically Processed M-50
Bar Code: N-2

Number of Specimens Tested = 8 Number Failed = 8 N-2

Life of Specimen (Millions of Cycles)	Failure Code
10.02	F
11.82	F
11.99	F
18.58	F
39.34	F
51.01	F
64.63	F
81.09	F

(F=Failed; D=Discontinued)

Naval Air Propulsion Center
Trenton, N.J.

Weibull Analysis Parameter Comparison
of Confidence Numbers for L(10) Life and Mean Life
for Rolling Contact Fatigue Data

R.C.F. Evaluation of Thermo-Mechanically Processed M-50

	L(10)LIFE	Mean Life	Weibull Slope	No. of Failures	X-Mean Stan. Dev. Squared
A-1	3.90	33.66	1.037	8	2.800
F-2	6.87	45.81	1.155	9	0.997 3.400
K-3	4.37	17.80	1.493	10	0.934 2.631
N-2	6.43	38.65	1.212	8	0.537 3.294 0.712

LIST OF REFERENCES

1. Bres, E. V., The Heat Treatment Response of Thermomechanically Processed M-50 Steel, M.S.M.E. Thesis, Naval Postgraduate School, Monterey, California, 1983.

2. NASA TM X-71441, Rolling-Element Bearings: A Review of the State of the Art, by W. J. Anderson and E. V. Zaretsky, pp. 1-12, 1973.

3. NASA Conference Publication 2210, Present Technology of Rolling-Element Bearings, by R. J. Parker, p. 40, 1983.

4. Larson, K. R., Jr., Thermomechanical Processing of M-50 Steel, M.S.M.E. Thesis, Naval Postgraduate School, Monterey, California, 1983.

5. Brick, R. M., Pense, A. W., and Gordon, R. B., Structure and Properties of Engineering Materials, 4th ed., pp. 305-307, McGraw-Hill Book Company, 1977.

6. Bridge, J. E., Jr., Maniar, G. N., and Philip, T. V., "Carbides in M-50 High Speed Steel," Metallurgical Transactions, v. 2, pp. 2209-2214, August 1971.

7. Metals Handbook, 9th ed., v. 3, pp. 421-425, American Society for Metals, 1980.

8. Metals Handbook, 9th ed., v. 1, pp. 110-111, American Society for Metals, 1978.

9. Metals Handbook, 9th ed., v. 4, pp. 599-610, American Society for Metals, 1981.

10. Popgoshev, D. and Valori, R., "Rolling Contact Fatigue Evaluation of Advanced Bearing Steels," Rolling Contact Fatigue Testing of Bearing Steels, ASTM STP 771, J.J.C. Hoo, Ed., American Society for Testing and Materials, pp. 342-357, 1982.

11. Metals Handbook, 8th ed., v. 11, p. 9, American Society for Metals, 1976.

12. Metals Handbook, 8th ed., v. 8, p. 64, American Society for Metals, 1973.

13. McNelley, T. R., et al., "The Effect of Prior Heat Treatments on the Structure and Properties of Warm-Rolled AISI 52100 Steel," Metallurgical Transactions, v. 14, pp. 1427-1433, July 1983.

14. Wells, M. G. H. and Lherbier, L. W., Eds., Processing and Properties of High Speed Tool Steels, p. 60, Metallurgical Society of AIME, 1980.

15. Ibid., p. 22.

16. Johnson, L. G., The Statistical Treatment of Fatigue Experiments, Elsevier, Amsterdam, London, New York, 1964.

17. Zaretsky, E. V., NASA Lewis Research Center, Cleveland, Oh., and Butterfield, F. A., III, Naval Postgraduate School, Monterey, California, private communications, November 1984.

18. NASA TP-2189, Effect of Carbide Distribution on Rolling-Element Fatigue Life of AMS 5749, by R. J. Parker and E. N. Bamberger, pp. 1-9, 1983.

19. NASA TN D-6835, Effect of Carbide Size, Area, and Density on Rolling-Element Fatigue, by J. L. Chevalier and E. V. Zaretsky, pp. 1-17, 1972.

20. Chevalier, J. L., Zaretsky, E. V., and Parker, R. J., "A New Criterion for Predicting Rolling-Element Fatigue Lives of Through-Hardened Steels," Journal of Lubrication Technology, v. 95, pp. 287-293, July 1973.

21. NASA TP-1060, Effect of Double Vacuum Melting and Retained Austenite on Rolling-Element Fatigue Life of AMS 5749 Bearing Steel, by R. J. Parker and R. S. Hodder, pp. 5-7, 1977.

22. Kerrison, G. D. and MacPherson, P. B., Metallurgical Aspects of Rolling Fatigue: A Literature Survey, Westland Helicopters Limited, p. 16, December 1977.

23. Maurer, R. E., SKF Technology Services, SKF Industries, Inc., King of Prussia, Pennsylvania and McNelley, T. R., Naval Postgraduate School, Monterey, California, private communication, November 1984.

24. Metals Handbook, 8th ed., v. 10, p. 17, American Society for Metals, 1975.

25. Tallian, T. E., discussion on Bamberger, E. N., "The Effect of Ausforming on the Rolling Contact Fatigue Life of a Typical Bearing Steel," Journal of Lubrication Technology, pp. 73-74, January 1967.

26. Bamberger, E. N., "The Effect of Ausforming on the Rolling Contact Fatigue Life of a Typical Bearing Steel," Journal of Lubrication Technology, pp. 63-72, January 1967.

27. NASA TN D-4954, Rolling-Element Fatigue Life of Ausformed M-50 Steel Balls, by R. J. Parker and E. V. Zaretsky, pp. 1-13, 1968.

28. Zaretsky, E. V., discussion on Bamberger, E. N., "The Effect of Ausforming on the Rolling Contact Fatigue Life of a Typical Bearing Steel," Journal of Lubrication Technology, pp. 74-75, January 1967.

29. NASA TN D-259, Rolling-Contact Fatigue Life of a Crystallized Glass Ceramic, by T. L. Carter and E. V. Zaretsky, pp. 1-15, 1960.

INITIAL DISTRIBUTION LIST

		No. Copies
1.	Defense Technical Information Center Cameron Station Alexandria, Virginia 22314	2
2.	Library, Code 0142 Naval Postgraduate School Monterey, California 93943	2
3.	Department Chairman, Code 69 Department of Mechanical Engineering Naval Postgraduate School Monterey, California 93943	1
4.	Dr. T. R. McNelley, Code 69 Department of Mechanical Engineering Naval Postgraduate School Monterey, California 93943	5
5.	Shipyard Commander Philadelphia Naval Shipyard (Attn: LT F. A. Butterfield, III, USN) Philadelphia, Pennsylvania 19112	2
6.	Commanding Officer Naval Air Propulsion Center (Attn: Mr. Dan Popgoshev) P.O. Box 7176 Trenton, New Jersey 08628	2
7.	Commander Aero Propulsion Laboratory (Attn: Mr. Ron Dayton) Air Force Wright Aeronautical Laboratories Air Force Systems Command Wright-Patterson Air Force Base, Ohio 45433	2
8.	Mr. Erwin V. Zaretsky NASA Lewis Research Center Cleveland, Ohio 44135	1
9.	LT Elizabeth V. Bres, USN 8187 Lariat Trail, N.W. Bremerton, Washington 98310	1

10. LCDR Keith R. Larson, Jr., USN 1
c/o Mr. K. R. Larson, Sr.
1323 Maple Street
Niles, Michigan 49120

END

FILMED

6-85

DTIC